

DEPARTMENT OF CHEMISTRY, UNIVERSITY OF JYVÄSKYLÄ  
RESEARCH REPORT No. 24

# THE ION EXCHANGE AND ADSORPTION PROPERTIES OF SPHAGNUM PEAT UNDER ACID CONDITIONS

BY  
MARTTI AHO

Academic Dissertation  
for the Degree of  
Doctor of Philosophy



Jyväskylä, Finland 1986  
ISBN 951-679-533-1  
ISSN 0357-346X

DEPARTMENT OF CHEMISTRY, UNIVERSITY OF JYVÄSKYLÄ  
RESEARCH REPORT No. 24

# THE ION EXCHANGE AND ADSORPTION PROPERTIES OF SPHAGNUM PEAT UNDER ACID CONDITIONS

BY  
MARTTI AHO

Academic Dissertation  
for the Degree of  
Doctor of Philosophy

To be presented by permission of the Faculty of  
Mathematics and Natural Sciences of the University  
of Jyväskylä for public examination in Auditorium  
S-212 May 16, 1986 at 12 o'clock noon



Jyväskylä, Finland 1986  
ISBN 951-679-533-1  
ISSN 0357-346X

**URN:ISBN:978-951-39-9969-8**  
**ISBN 978-951-39-9969-8 (PDF)**  
**ISSN 0357-346X**

**Jyväskylän yliopisto, 2024**

## PREFACE

The experimental work described in this publication was carried out at the Department of Chemistry, University of Jyväskylä, between 1978 and 1981. Since 1982 I have been employed at the Domestic Fuel Laboratory of the Technical Research Centre of Finland in Jyväskylä and the manuscript was written there during 1984.

I wish to express my sincere gratitude to my teacher at the University of Jyväskylä, Associate Professor Jouni Tumma-  
vuori, whose interest and encouragement were of great help throughout the course of the work.

My sincere thanks to Professor Jussi Valkonen, University of Jyväskylä, and Professor Rouse S. Farnham, University of Minnesota, U.S.A., for their encouragement and helpful comments on the manuscript, and to Docent Pertti Kokkonen, University of Oulu, and Dr. Timo Nyrönen, Vapo Oy, for undertaking a preliminary reading.

Thanks go as well to Dr. Kathleen Ahonen for improving the language of the manuscript and to Miss Ritva Nyysönen for preparing the typescript.

The support of this research by the Technical Research Centre of Finland is gratefully acknowledged.

To my wife and children I owe a great debt of gratitude for their support and understanding.

Jyväskylä, November 1985

Martti Aho

PREFACE

ABSTRACT	1
INTRODUCTION	3
1 REVIEW OF THE LITERATURE	4
1.1 Familiarization with peat	4
1.1.1 What is peat?	4
1.1.2 Decomposition in peat and some indication methods	4
1.1.3 Contents of major compounds and elements	7
1.1.4 Water in peat	8
1.2 Ion exchange in resins	9
1.2.1 Ion exchange mechanisms and affinity	9
1.2.2 Structure and selectivity	11
1.3 Ion exchange in peat and capacity determination	13
1.3.1 Important functional groups and compounds	13
1.3.2 Ion exchange mechanisms in peat	16
1.3.3 A method of determining the ion exchange capacity of ion exchange resins	20
1.3.4 Methods of determining the ion exchange capacity of peat	20
2 EXPERIMENTAL	22
2.1 Origin and quality of peat samples	22
2.2 Dissolution of the samples for chemical analysis	23
2.3 Stock solutions	23
2.4 Chemical analysis	25
2.4.1 Atomic absorption spectrophotometry	25
2.4.2 Induction-coupled plasma emission spectrometry	25
2.4.3 Infrared spectrometry	27
2.4.4 Flame photometry	27
2.4.5 Titrimetric methods	27
2.4.6 Spectrophotometric methods	27
2.4.7 Thermogravimetry	27

2.5	Methods for determining ion exchange capacities	28
2.5.1	Dynamic method	28
2.5.2	The properties of dynamical adsorption curves	29
2.5.3	Calculations from dynamical adsorption curves	30
2.5.4	Static method	31
3	RESULTS AND DISCUSSION	32
3.1	Elemental analysis	32
3.1.1	Sample groups 1 and 2	32
3.1.2	Sample group 3	32
3.2	Infrared spectrometry	35
3.2.1	Sample groups 1 and 2	35
3.2.2	Sample group 3	37
3.3	Thermogravimetry	38
3.3.1	Calculations	39
3.3.2	Sample groups 1 and 2	41
3.3.3	Sample group 3	45
3.4	Adsorption properties	47
3.4.1	Effects of experimental conditions on adsorption in column experiments	47
3.4.1.1	The mechanism of ion exchange	47
3.4.1.2	Effect of pH	48
3.4.1.3	Effect of flow rate	50
3.4.1.4	Effect of concentration	51
3.4.1.5	Effect of column height	52
3.4.1.6	Summary of the effects	53
3.4.2	The adsorption of representative amounts of ions on medium-moor peat	55
3.4.2.1	Results for six divalent transition metals and Pb <sup>2+</sup>	55
3.4.2.2	Results for other ions	59
3.4.2.3	Interpretation of the results	61

3.4.3	Adsorption of $\text{Cu}^{+2}$ , $\text{Sr}^{2+}$ , $\text{Ca}^{2+}$ and $\text{K}^{+}$ on pure <u>Sphagnum</u> peat species	65
3.4.3.1	Adsorption curves	66
3.4.3.2	Comparison of the adsorptions	69
3.4.3.3	Comparison with literature data	71
3.4.4	Relevance of sampling place	71
3.4.4.1	Adsorption behaviour	72
3.4.5	The effect of two pretreatment methods on adsorption properties of peat	75
3.4.5.1	Effect of freezing	75
3.4.5.2	Effect of extracting part of the long-chain hydrocarbons	76
3.4.6	Multi-cation experiments	77
3.4.6.1	Forcing-out experiment	78
3.4.6.2	Shaking experiments	80
3.4.7	Peat as a cation filter	81
3.4.7.1	Repeated use of a larger peat layer	82
	CONCLUSIONS	86
	REFERENCES	
	APPENDIX	

E R R A T A

page:	line:	is:	should be:
4	21	Bryales	<u>Bryales</u>
39	Eq. 18	A, E*, R, T	Comm.: explanations in Table VIII
40	Eq. 21	$= \ln [1/(1-\alpha)]$	$= \ln [1/(1-\alpha)]$
40	Eqs. 24,26	$e^{-E^*/RT}$	$e^{-E^*/RT}$
59	17	ph	pH
65	13	Ag <sup>2+</sup> , Co <sup>2+</sup>	Ag <sup>+</sup> , Co <sup>2+</sup>
86	27	... filter, like ion exchange resins.	... filter.



## ABSTRACT

The effects of experimental conditions on ion exchange capacity of low- and medium-moor Sphagnum peat were tested in column-type experiments. The ion exchange mechanisms of the samples differed, and proton-cation exchange was more prominent with the low-moor sample. The typical adsorption curve consisted of a region with high adsorption level (> 99.5 %) and a descending region where the slope obeyed first order kinetics. The capacity of the low-moor sample was nearly twice that of the medium-moor sample, which was also indicated by the infrared spectra of the samples. pH had a strong influence on the adsorption in the range 2.0 - 4.9: increase of pH increased the adsorption. Concentration of the test solution was of smaller significance although increasing capacity was observed with increasing cation concentration. Column height and flow rate were of little or no importance in the studied range because of the rapidity of the adsorption.

Adsorption experiments with representative amounts of ions on medium-moor Sphagnum peat at pH 3.0 - 3.3 revealed that with divalent transition metals the adsorption affinity obeys the complex stability order published in the literature. Trivalent cations were strongly adsorbed, as was expected. With alkalies and alkaline earths the adsorption capacity usually decreased with increasing ratio of molecular weight to charge.  $\text{Sr}^{2+}$  was an exception, proving the high selectivity of peat at pH 3.0 - 3.3. The adsorption of anions was extremely weak.

The pure Sphagnum peat species differed in their adsorption properties. S. Fuscum was the strongest adsorber for most ions. Measurement of IR spectra proved to be a good method for rough estimation of capacity of a peat.

The sampling place is of relevance to adsorption behaviour, as was shown with low-moor samples from three production areas.

Pretreatment by freezing strengthened the adsorption by elongating the region of high adsorption level if the water content was 95 % at freezing. Extraction of the long-chain hydrocarbons may increase the capacity if the sample contains large amounts of those hydrocarbons.

Like an ion exchange resin, peat can be used repeatedly as a cation adsorber, although its capacity is lower. It behaves like selective, complexing resin.

## INTRODUCTION

The purpose of this work was to determine the ion exchange and adsorption properties of Sphagnum-type peat in natural state and harvested state, suitable for further refining. Pretreatment was avoided because it destroys the original state of the peat: peat is not only protonated by acid but dissolution of certain compounds takes place as well. Experiments on the influence of freezing and of one type of extraction on adsorption were nevertheless made at the end of the study.

The adsorption properties of peat have been investigated to some degree before this work but the number of publications on the subject is limited. This is the first study that embraces a thorough series of experiments by column method with a flow of test solution through a peat layer.

The work was started by measurement of the effects of experimental conditions on adsorption on two different samples of Sphagnum peat. The next phase was study of the adsorption of representative amounts of ions on a medium-moor peat sample from single cation test solutions. Because milled peat contains mixtures of peat species the work was continued with a study of the adsorption properties of individual Sphagnum peat species. The influence of sampling place was of interest too, and tests were performed with low-moor peat samples from three production areas. Adsorption experiments after mild pretreatment were carried out with two peat species, as also multi cation experiments. Finally, the peat layer was used like an ion exchange resin to test its properties as a cation filter.

The results provide basic information about peat, important for its application in agriculture, filtration, refining and combustion. The results have been published earlier in five articles, which are referred to in the text.

## 1 REVIEW OF THE LITERATURE

### 1.1 Familiarization with peat

#### 1.1.1 What is peat?

Peat is formed when wetland plants moulder incompletely producing species that can be preserved in humic conditions. Because the formation of plant residues is only slightly faster than their complete mouldering, peat is formed at the rate of only 0.1 - 1.2 mm per year /1/.

Geographical location, average humidity and temperature all influence the type of wetland. The main wetland types in Europe from south to north are: 1) bogs in the southern part of the hardwood forest zone, 2) bogs within the hardwood forest zone and in the southern part of the softwood forest zone, 3) bogs in the central and northern parts of the softwood and birch forest zone, and 4) arctic wetlands. If climate differs at the same latitude, the wetland type may vary markedly /2/.

In Finland, peat is classified and named according to the botanical names of the plants forming it. Sphagnum peat contains pure Sphagnum species or contains, in addition to Eriophorum Vaginatum, Cares, or Woody species. Carex peat contains pure Carex species and sometimes, in addition, Eriophorum Vaginatum, Woody, or Bryales species. Bryales peat contains pure Bryales species or Bryales and Carex species. Woody peat contains a mixture of Woody parts and Sphagnum and Bryales species. Peats contain as well many minor compounds. For example traces of horsetail (Equisetum) and common reed (Phragmites) can be found in Carex peat /3/.

#### 1.1.2 Decomposition in peat and some indication methods

Decomposition is an important process in peat. Several degrees of humification can be observed in peat bogs. Generally, the degree of humification increases

Table I. Classification of peat by degree of humification, by von Post system /7/.

Scale description	Scale description
H1 Completely undecomposed peat which, when squeezed, releases almost clear water. Plant remains easily identifiable. No amorphous material present.	H6 Moderately strongly decomposed peat with a very indistinct plant structure. When squeezed, about one-third of the peat escapes between the fingers. The residue is strongly pasty but shows the plant structure more distinctly than before squeezing.
H2 Almost completely undecomposed peat which, when squeezed, releases clear or yellowish water. Plant remains still easily identifiable. No amorphous material present.	H7 Strongly decomposed peat. Contains a lot of amorphous material with very faintly recognizable plant structure. When squeezed, about one-half of the peat escapes between the fingers. The water, if any is released, is very dark and almost pasty.
H3 Very slightly decomposed peat which, when squeezed, releases muddy brown water, but for which no peat passes between the fingers. Plant remains still identifiable and no amorphous material present.	H8 Very strongly decomposed peat with a large quantity of amorphous material and very dry indistinct plant structure. When squeezed, about two-thirds of the peat escapes between the fingers. A small quantity of pasty water may be released. The plant material remaining in the hand consists of residues such as roots and fibres that resist decomposition.
H4 Slightly decomposed peat which, when squeezed, releases very muddy dark water. No peat is passed between the fingers but the plant remains are slightly pasty and have lost some of their identifiable features.	H9 Practically fully decomposed peat in which there is hardly any recognizable plant structure. When squeezed, almost all of the peat escapes between the fingers as a fairly uniform paste.
H5 Moderately decomposed peat which, when squeezed, releases very "muddy" water with also a very small amount of amorphous granular peat escaping between the fingers. The structure of plant remains is quite indistinct, although it is still possible to recognize certain features. The residue is strongly pasty.	H10 Completely decomposed peat with no discernible plant structure. When squeezed, all the wet peat escapes between the fingers.

with increasing sampling depth. The degree of humification is determined as the ratio of the amorphous humic substances to the plant cells and fibres in peat.

The most widely used indication methods in Europe have been developed by von Post /4/ and Pjavitshenko /5/. In the method of von Post the analysis is carried out by pressing the peat sample in clenched hand. A detailed description is given in table I.

Pjavitshenko's method /5/ is based upon a density analysis: the greater the density of the sample, the greater is the degree of humification. The densities of both the amorphous part and the fibrous part are needed for calculations. Pjavitshenko introduces the following formulas:

$$H = \frac{d - d_0}{K} \quad (1)$$

where

H = per cent of humification

d = density of the sample

$d_0$  = density of the fibrous part of the sample

$$K = \frac{d_n - d_0}{100} \quad (2)$$

where

$d_n$  = density of the amorphous part of the sample

The density values are those of a dry and ashless sample.

In the standard method of USSR /6/ the amorphous part is first coagulated and then separated from the fibrous part by wet sieving of the sample twice in a centrifuge. The humification per cent is calculated from the volume of the sedimented part of the sample.

In the United States peat is classified into the three categories of Fibric, Hemic and Sapric depending on the degree of humification /7/.

Because of the complicated structure of peat the methods give only approximate information about mouldering. Von Post's method is most widely used, in Europe as it is both simple and rapid.

### 1.1.3 Contents of major compounds and elements

The major compounds in peat and their relative amounts at various degrees of humification are shown in Table II.

Table II. The relative amounts of major compounds in peat /8/.

Compound	Degree of humification by von Post		
	1 - 2 %	5 - 6 %	9 - 10 %
Cellulose	15 - 20	5 - 15	-
Hemicellulose	15 - 30	10 - 25	0 - 2
Lignin	5 - 40	5 - 30	5 - 20
Humic substances	0 - 5	20 - 30	50 - 60
Bitumens	1 - 10	5 - 15	5 - 20
Nitrogen (as protein)	3 - 14	5 - 20	5 - 25

The amounts of cellulose and hemicellulose decrease and the percentage of humic substances increases with increasing humification. The increasing tendency can also be seen with bitumens (mainly consisting of waxes and resins) and nitrogen compounds.

Figure 1 shows the concentrations of major elements at various degrees of humification.

The amounts of carbon, nitrogen and inorganic compounds increase and oxygen concentration decreases with increasing humification. Hydrogen content remains nearly constant.

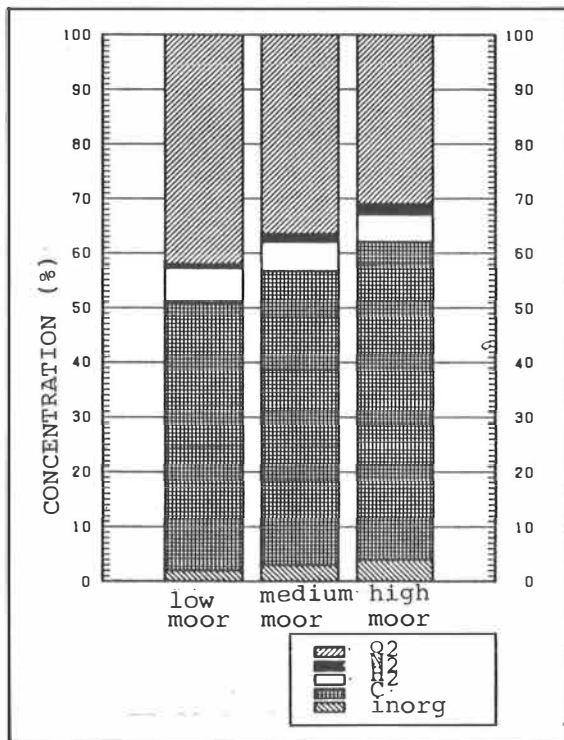


Figure 1. The major element contents in peat /8/.

#### 1.1.4 Water in peat

Virgin bog peat always has a high water content: about 90 % of the total weight.

Several theories have been presented concerning water binding in peat. One of the most attractive is that of Oswald /9/. According to his theory, water in large porous parts of the structure is most readily released. Water in narrow capillaries can be released under high pressure. Water on the surface of negatively charged colloids can be released by coagulants. Unmouldered cells contain water that is difficult to force out except under very high pressure. And the water bound chemically in the structure can be released only by heating the sample.



## 1.2 Ion exchange in resins

### 1.2.1 Ion exchange mechanisms and affinity

The ion exchange phenomenon involves redistribution of ions A and B (called counterions) between solution and ion exchanger by diffusion. The process is not a true chemical reaction. Counterion diffusion is subject to the restriction of electroneutrality: as ions of the species A move into the solution a stoichiometrically equivalent amount of species B must move into the ion exchanger to balance the electric charges of the fixed ionic groups.

The rate-controlling step was first shown by Boyd et al. /10/ to be diffusion, either in the ion exchanger particle itself or in an adherent stagnant liquid layer, or film. In an intermediate range of conditions both mechanisms may affect the rate.

In the film model, first introduced by Nernst /11/, it is assumed that a completely stagnant film with a sharp boundary is separating the particle surface of the exchanger from the solution. The thickness of the hypothetical Nernst film is related to the Sherwood number (in engineering use) by the equation

$$\delta = 2 r_0 / Sh \quad (3)$$

where

$r_0$  is the radius of the ion exchanger particle

$$Sh = 2 + 0.66 Sc^{1/3} Re^{1/2}, Re < 500 \quad /12/ \quad (4)$$

where

Re = Reynold's number

Sc = Schmidt's number

$$\text{Re} = d_p \left| w_f - w_s \right| \rho / \eta \quad (5)$$

where

$w_f, w_s$  = the velocities of the fluid and solid particle, m/s

$d_p$  = diameter of the solid particle, m

$\rho$  = density of the fluid, kg/m<sup>3</sup>

$\eta$  = dynamical viscosity of the fluid, Ns/m<sup>2</sup>

$$\text{Sc} = \eta / (D_v \rho) \quad (6)$$

where

$D_v$  = diffusion coefficient (volumetric), m<sup>2</sup>/s

As film and particle diffusion are sequential steps, the slower of the two is rate-controlling. The rate-controlling step can be predicted theoretically by the formula

$$X = \frac{\bar{C} \bar{D} \delta}{C D r_0} (5 + 2 \alpha_{A/B}) \quad (7)$$

where

$\bar{C}, C$  are the total concentrations of the counterions in ion exchanger and solution, mole/dm<sup>3</sup>

$D, D$  are the diffusion coefficients in exchanger and solution, m<sup>2</sup>/s

$\alpha_{A/B}$  is the separation factor

If the value of the formula (7) is  $\gg 1$ , the reaction is controlled by film diffusion. If the value is  $\ll 1$ , the reaction is controlled by particle diffusion.

The best method for distinguishing experimentally between particle and film-diffusion control is by interruption test /13/, in which the ion exchange reaction is stopped by removing the particles from the solution for a short period of time. Only with particle diffusion control is the exchange rate higher upon reimmersion than at the moment of interruption, because internal concentration gradients have time to level out.

In most theories that have been published it is assumed that the effective surface charge of the ion, determined by the ratio of the charge of the ion to its hydrated radius, and the type of the exchanger determine the adsorption affinity. In Eisenman's /14/ theory the hydration of ions is recognized as of key importance. However hydration is considered primarily in terms of the energetics rather than in terms of radius or volume of hydrated ions. Electrostatic interactions are regarded as the primary source of irregularities.

### 1.2.2 Structure and selectivity

Ion exchanger resins consist of three-dimensional polymeric or crystalline networks carrying fixed ionic groups and containing mobile exchangeable counterions (coions) having charges of opposite sign to the fixed groups. Typical functional groups in cation exchangers are sulfonic acid, phenolhydroxyl and carboxyl groups. Typical corresponding groups in anion exchangers are various ammonium derivatives.

There are roughly three parameters defining the structure of an ion exchange resin: 1. The nature of the exchange grouping, 2. the degree of cross-linking, 3. the number of exchange groupings per unit amount of exchanger, usually defined by special ion exchange capacity, i.e. the number of milliequivalents of fixed exchange groupings per one gram of exchanger in a given ionic form /15/.

If we consider the case of ions  $X^{n+}$  and  $Y^{m+}$  when  $n = m = 1$ , the corrected selectivity coefficient is of the form

$$K'_{Y/X} = \frac{\bar{X}_Y a_x}{X_x a_y} \quad (8)$$

where

$\bar{X}_x, \bar{X}_y$  = the equivalent fractions of the counterions in the exchanger

$a_x, a_y$  = the corresponding activities of the ions in solution

The activity is assumed to be constant in the solid part.

If  $m = 2$  and  $n = 1$  the situation is more complicated, for the definition of  $X$  is then uncertain. There are two possibilities: to calculate  $X$  as equivalent or as mole fraction. Assuming that the relative amounts of  $X^{n+}$  and  $Y^{m+}$  in the exchanger depend on the total activity of  $X^{n+}$  and  $Y^{m+}$  as well as on their relative activities and that the activity coefficient is unity, the selectivity coefficient is of the form

$$K'_{X/Y} = \frac{\bar{X} Y^{2+}}{(\bar{X}_{x+})^2} \frac{m (X_{x+})^2}{X Y^2} \quad (9)$$

where

$\bar{X}_x, \bar{X}_y$  the equivalent fractions of the counterions in the exchanger

$X_x, X_y$  = the corresponding concentrations of the ions in the solution

$m$  = the total concentration of  $X$  and  $Y$  in the solution, expressed as mole/dm<sup>3</sup>

The effect of cross-linking of the sulfonated cation resin on the selectivity coefficients of the Na/H system is shown in Figure 2 /15/.

The selectivity coefficient  $K'_{Na/H}$  increases with increasing cross-linking, if the value of  $\bar{X}_{Na}$  is not too high.

Another example of the significance of cross-linking of fully sulfonated resin is the affinity order of the alkalis on the resin. With low degree of cross-linking the order is Cs > K > Na > Li. With high degree of cross-linking the affinity order is K > Na > Li > Cs.

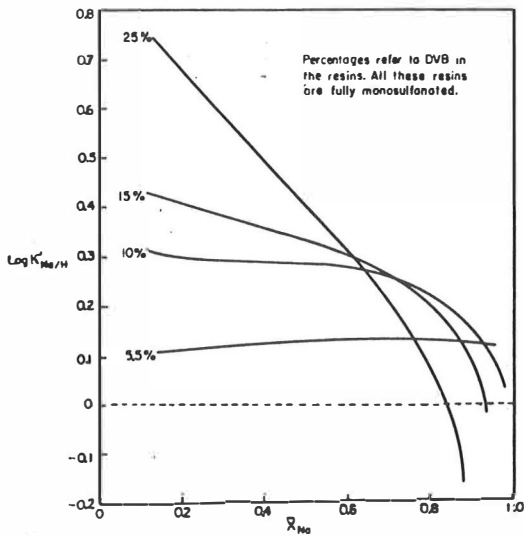


Figure 2. Sodium-hydrogen selectivity on monosulfonated polystyrene resin. DVB value = degree of cross-linking.

### 1.3 Ion exchange in peat and capacity determination

#### 1.3.1 Important functional groups and compounds

Peat is an active ion exchange material. In its sorption and ion exchange properties it is similar to natural zeolites, silicate exchangers, natural polymers (celluloses) and certain types of resins /16/.

The distribution and number of functional groups determine the ion exchange behaviour of peat, and it behaves differently from synthetic ion exchange resins. In peat the reactive groups contain coordinatively non-saturated oxygen atoms and easily mobile electrons along the chain of conjugated bonds. This makes possible the formation of chelate-type complexes. Additional coordination bonds with neighbouring oxygen-containing groups may be created at sorption. These coordination bonds are important for ion-exchange properties of peat and especially for its selectivity /17/.

The humic and fulvic acids, easily hydrolyzed substances (poly-uronides and uronic acids), and lignin to a certain extent, are the important chemical compounds in ion exchange in peat. The exchange may take place in the -COOH groups, phenolic hydroxyls and heterocyclic groups =NH, -SH. Both neutral exchange and H exchange with cation occur. The OH-exchange is of secondary importance /17/.

The structures of the important chemical compounds of peat are extremely complicated and the published structures of any one compound are not always identical. They do, however, indicate the location of the important functional groups.

The most important structural unit in the lignin molecule is the phenylpropyl group. The relative amounts of functional groups are dependent on the origin of the lignin. Figure 3 shows how three structural units can be bound together. Actually, the molecule consists of a complicated network of chains containing phenylpropyl units /19/.

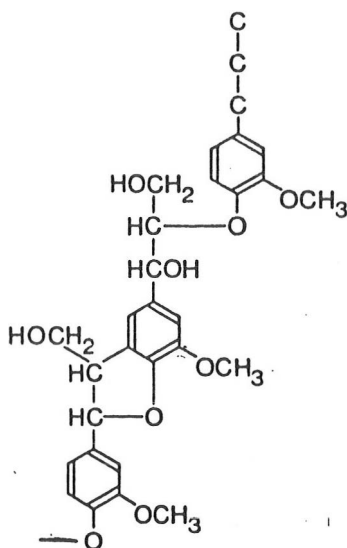


Figure 3. A small part of a lignin molecule /19/.

Humic substances are mouldering products of lignin and likewise have a polyphenol network structure. The dominant functional group is the carboxyl group and there are a smaller number of methoxyl groups than in lignin. The structure of the humic acid molecule is complicated and the structural analysis difficult. Two different solutions have been presented in the literature: the model of Fuchs /20/ shown in Figure 4 and the corresponding proposition of Dragunov in Figure 5.

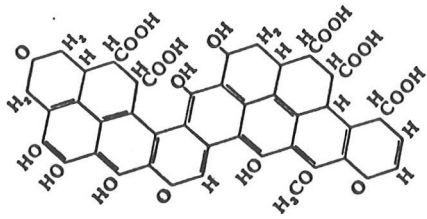


Figure 4. The humic acid molecule, Fuchs model /20/.

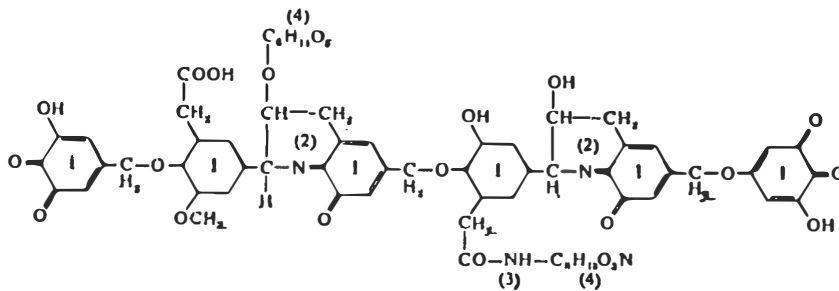


Figure 5. The humic acid molecule, Dragunov model /20/.

In the fulvic acid molecule the structural units are bound together by hydrogen bonds, which cause flexibility in the molecule (Figure 6) /21/.

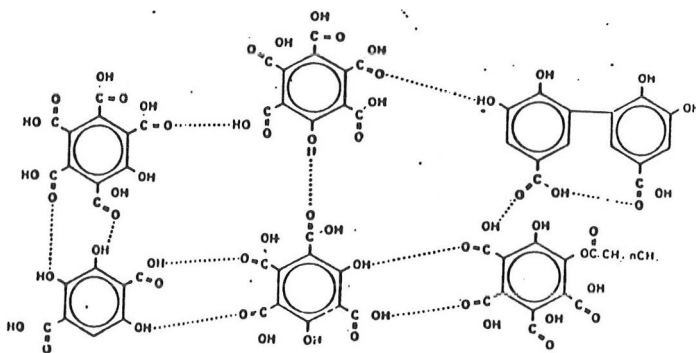


Figure 6. Partial structure of the fulvic acid molecule /21/.

### 1.3.2 Ion exchange mechanisms in peat

Bunzl studied ion exchange in peat in a series of kinetic experiments. He added cation ( $Pb^{2+}$ ) continuously /18/ and in small portions /16/ to a vessel containing a water suspension of  $H^+$ -saturated peat. In both cases the rate-controlling step in the ion exchange reaction turned out to be film diffusion, as concluded from the results of interruption tests and calculations.

Bunzl /22/ gives the following general equation for a film diffusion controlled, ion-exchange process:

$$\frac{dX_1}{dt} = \frac{R}{C} \cdot \frac{\alpha_2 r_{1c} c_1 z_1 [1-X_1] - z_2 c_2 r_{2c} X_1}{\alpha_2 D_2 [1-X_1] + D_1 X_1} \quad (10)$$

where

- $X_1$  =  $z_1 C_1 / C$
- $z_1$  = signed valences of the ions
- $C_1$  = concentration of the ion in the ion exchanger (mole/dm<sup>3</sup>)
- $C$  = total cation exchange capacity of the sample (meq/cm<sup>3</sup>)
- $R$  =  $\bar{F} D_1 D_2 / \sqrt{V} \delta$



- $\bar{F}/\bar{V}$  = surface-to-volume ratio of the ion exchanger, for spherical particles =  $3/r$  ( $r$  = particle radius)
- $D_1, D_2$  = diffusion coefficients, which are functions of the four diffusion coefficients  $D_{ij}$ , describing isothermal diffusion in the corresponding ternary electrolyte solution involving the counterions 1 and 2 and the common coion 3.
- $\delta$  = film thickness
- $r_{1c}, r_{2c}$  = stoichiometric coefficients for ionization
- $\alpha_{\frac{1}{2}}$  = equivalent separation factor
- $c_1$  = concentration of the ion 1 in the reaction vessel (mole/dm<sup>3</sup>)
- $c_2$  = concentration of the ion 2 in the reaction vessel (mole/dm<sup>3</sup>)

In the continuous addition experiments carried out by Bunzl the peat particles are completely saturated with the counter ions 2 ( $H^+$ ) at time  $t=0$ . After the process has begun of adding  $Pb^{2+}$  ions to the reaction vessel, using a small volume of the solution compared with the suspension in the vessel, the situation can be described by the formula

$$c(t) = \frac{n N t}{V_0} = a t \quad (11)$$

where

- $c(t)$  = the sum of the concentrations of the two ions in the reaction vessel (mole/dm<sup>3</sup>)
- $nN$  = the feed rate of counterion 1 ( $Pb^{2+}$ ) (mole/(dm<sup>3</sup>s))
- $V_0$  = volume of the solution in the reaction vessel, (dm<sup>3</sup>)
- $t$  = time (s)

Taking into account that all ions 2 leaving the ion exchanger have to appear in the solution and starting from equation 10, Bunzl arrived at a new differential equation

$$\frac{dQ}{dt} = \frac{R}{C} \cdot \frac{\alpha_1 [at - Cw X_1] [1 - X_1] - Cw X_1^2}{\alpha_2 D_2 [1 - X_1] + D_1 X_1} \quad (12)$$

where

$$w = \bar{V}/V_0$$

$\bar{V}$  = volume of the ion exchanger sample (cm<sup>3</sup>)

$Q$  = amount of the ions exchanged by the sample at time  $t$   
 =  $z_1 C_1 \bar{V}$  (meq)

$Q_\infty$  = total amount of ions which can be taken up by the  
 sample (meq)

Equation 12 describes the rate of ion exchange in a reaction vessel to which the counterions are added continuously at a constant feeding rate  $nN$ .

An analytical solution to Eq. 12 is impossible. To see how the rate of ion exchange depends on feed rate and the separation factor, Bunzl used the value of fractional attainment of equilibrium defined as

$$U = Q / Q_\infty \quad (13)$$

as a function of time using different values of feeding rate and separation factor and assuming reasonable values for the constants. The results are seen in Figure 7.

Three important characteristics of the rate curves in Figure 7 are as follows:

1. The curves have a characteristic sigmoidal shape, not observed in ion exchange processes to which the counterions are all added at the same time.

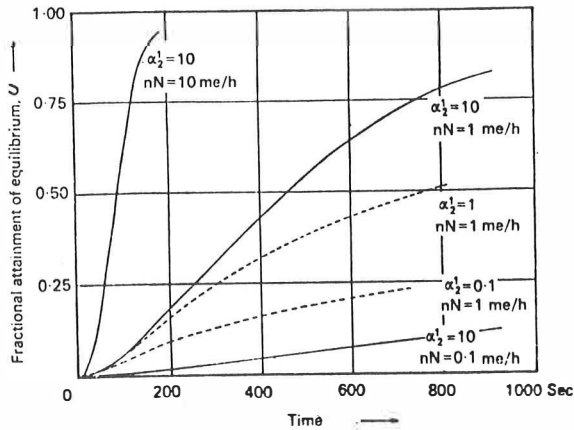


Figure 7. Kinetics of ion exchange during continuous addition of ions. Fractional attainment of equilibrium  $U$  as a function of time  $t$ , calculated according to Eq. 12. Parameters are the feed rate  $nN$  and the selectivity coefficient  $\alpha_1$ . The constants in Eq. 12 were selected as follows:  $V = 200$  ml,  $C = 2$  meq/ml,  $D_1 = 2 \cdot 10^{-5}$  cm<sup>2</sup>/sec,  $D_2 = 1 \cdot 10^{-5}$  cm<sup>2</sup>/sec,  $V = 0.1$  ml,  $F/V = 300$  (which corresponds to a particle radius of 0.01 cm),  $\delta = 2 \cdot 10^{-4}$  cm.

2. The rate of ion exchange increases with the feed rate (compare solid curves).
3. The more the added counterions are taken up in preference to the ions originally in the ion exchanger (increase in  $\alpha_1$ ), the faster the rate of ion exchange will be (compare dashed curves and second curve from top).

Also, the rate of ion exchange will be enhanced by all factors what increase the rate of film diffusion, namely the surface area of the ion exchanger, the rate of agitation and the temperature.

Bunzl /16/ also calculated the case of small successive addition of the cation. The starting equation was again that for a film-diffusion controlled, ion exchange process

(10). After plotting the curves on the basis of modified equation 10, using the separation factor as the parameter he found four important characteristics of the curves:

1. The initial rate of each differential ion exchange process is directly proportional to  $\Delta c$  (= the amount of ions 1 added) and to  $R'$  (= the surface-to-volume ratio of the ion exchanger). It is inversely proportional to the film thickness  $\delta$ , which is determined mainly by the rate of agitation in the reaction vessel.
2. The initial rate of each differential ion exchange reaction decreases if the ion exchanger contains initially more of the ion 1 to be taken up.
3. At a given initial composition of the ion exchanger and for given ions 1 and 2 (which determine the value of  $D_1/D_2$ ) the initial rate of the differential ion exchange process is faster if  $\alpha_1$  is high (= if ions 1 are taken up preferentially compared with ions 2).
4. The initial rate of each differential ion exchange process increases as  $D_2/D_1$  decreases.

### 1.3.3 A method of determining the ion exchange capacity of resins

The capacity is usually determined by balancing the ion test solution with a known amount of resin. Typical balancing time is 24 hours. The ion uptake is expressed as curves where the amount of bound ion is as y axis and pH is as x axis. Kinetic measurements are needed to estimate the delay to complete complexing.

### 1.3.4 Methods of determining the ion exchange capacity of peat

Puustjärvi /23/ has developed a conversion - titration method for determination of the ion exchange capacity of peat. In this method peat is first shaken with  $0.5 \text{ mol/dm}^3$  HCl to convert the ion exchange groups to  $\text{H}^+$  form. After

removal of excess acid the sample is treated with concentrated Ba (OOCCH<sub>3</sub>)<sub>2</sub> solution to replace H<sup>+</sup> with Ba<sup>2+</sup>. The released H<sup>+</sup> ions (as H<sub>3</sub>O<sup>+</sup>) are titrated with 0.1 mol/dm<sup>3</sup> NaOH solution and the result is calculated as milliequivalent per 100 g of air-dried peat. This method is easy to perform in small laboratories but it does not give information about reaction speeds and adsorption profiles.

Bunzl /16, 18/ has developed a kinetic conversion - pH-measurement method. The first step is similar conversion to H<sup>+</sup> form as in the method of Puustjärvi. The ion exchange reaction between H<sup>+</sup> and Pb<sup>2+</sup> is followed by pH measurement on the reasoning that one Pb<sup>2+</sup> ion releases two H<sub>3</sub>O<sup>+</sup> ions during adsorption. The method is very informative.

The ion exchange groups are not completely protonated in natural peat and after addition of acid the sample is not in its original form. An extreme example of conversion is the method of Lettinga et al. /24/ in which the moist peat is treated with 98 % H<sub>2</sub>SO<sub>4</sub> to ensure that protonation is complete. The appearance of the sample after the treatment is very different from what it was before. To avoid alternation in the structure of the peat, many researchers have measured the adsorption capacity of peat in natural state.

Bergseth /25/ suggests a method in which the peat sample is shaken with concentrated Sr (OOCCH<sub>3</sub>)<sub>2</sub> solution at pH 7. The strontium concentration in peat is then measured by X-ray fluorescence spectrometry for determination of the ion exchange capacity.

In the method of Broadbent et al. /26/ the capacity is determined by shaking the sample with barium acetate solution. In a second step, Ba<sup>2+</sup> is released with HCl. Barium is determined in the solution by flame photometry or gravimetry.

Sapek /27/ uses a kinetic method, following the copper adsorption on peat with an electrode selective for Cu<sup>2+</sup> ion.

## 2 EXPERIMENTAL

### 2.1 Origin and quality of peat samples

The peat samples studied can be divided into five groups according to the purpose of the substudy they were used in. The groups, with the degree of humification of the sample reported according to von Post's scale H1 - H10 /4/, are as follows:

- Group 1. Study of the effects of experimental conditions on adsorption in column experiments. Samples: Milled peat sample containing a mixture of Sphagnum peats, H5-6, from Rastunsuo production area, and a low-moor peat sample containing a mixture of Sphagnum peats, H1-2, from Haukineva production area.
- Group 2. Adsorption study of the representative amounts of ions in a particular peat. Sample: Milled peat sample containing a mixture of Sphagnum peats, H5-6, from Rastunsuo production area.
- Group 3. Adsorption study of pure Sphagnum peat species. Samples: S. Cuspidata H1-2, S. Palustria H1-2, S. Fuscum H2, S. Cuspidata H3, and S. Fuscum H3. The samples were collected from Central Finland.
- Group 4. Comparison of milled peat samples from various sampling places. Samples: Mixtures of Sphagnum species: H1-2 peats from Konnunsuo, Aitoneva and Haukineva, and H4-6 peat from Konnunsuo production area.
- Group 5. Adsorption study on frozen and extracted peats. Samples: As in group 2, plus Konnunsuo H4-6 (group 4).

The samples were kept in closed plastic bags in natural humidity.

## 2.2 Dissolution of the samples for chemical analysis

Dissolution of the dried (103 °C, 24 h) and milled samples was carried out in a PTFE combustion vessel developed for the purpose /28, 29/. The combustion solution (mixtures of pro analyse acids) was either 6:4:1 HF (40 %) - HNO<sub>3</sub> (65 %) - HClO<sub>4</sub> (70 %) or 4:1 HNO<sub>3</sub> (65 %) - HClO<sub>4</sub> (70 %) depending on the ion to be determined. If the ion formed precipitates with F<sub>2</sub><sup>2-</sup>, the latter solution was used. The sample weight, volume of the wet combustion solution, treatment time and temperature were with the former solution 0.8 g, 18 cm<sup>3</sup>, 3.5 h, 140 °C and with the latter solution 0.5 g, 10 cm<sup>3</sup>, 2 h, 130 °C. The samples were diluted after wet combustion as follows: HF- HNO<sub>3</sub>-HClO<sub>3</sub> to 100 cm<sup>3</sup> with saturated H<sub>3</sub>BO<sub>3</sub> solution, HNO<sub>3</sub>- HClO<sub>4</sub> to 50 cm<sup>3</sup> with distilled water. The standard solutions contained corresponding amounts of the acid mixtures.

## 2.3 Stock solutions

The stock solutions were prepared from pro analyse reagents, mostly nitrates. A suitable amount of acid, corresponding in type to the anionic part of the reagent, was added to prevent precipitation as hydroxide. The concentrations of the stock solutions were confirmed by a recommended method for the particular element.

More information about the stock solutions is given in Table III.

Table III. Stock solutions.

Ion	Reagent	Confirmative analysis	Concentration (mg/dm <sup>3</sup> )
Cr <sup>3+</sup>	CrCl <sub>3</sub> x6H <sub>2</sub> O	potentiometric titration with Ce <sup>4+</sup>	5310 /30/
Zn <sup>2+</sup>	ZnSO <sub>4</sub> x7H <sub>2</sub> O	titration with EDTA	1055
Hg <sup>2+</sup>	HgCl <sub>2</sub>	electrolysis	999
Cd <sup>2+</sup>	Cd(NO <sub>3</sub> ) <sub>2</sub> x4H <sub>2</sub> O	titration with EDTA	
		electrolysis	1003
Pb <sup>2+</sup>	Pb(NO <sub>3</sub> ) <sub>2</sub>	titration with EDTA	
		electrolysis	19900
Ni <sup>2+</sup>	Ni(NO <sub>3</sub> ) <sub>2</sub> x6H <sub>2</sub> O	gravimetric with dimethylglyoxime	997
Co <sup>2+</sup>	Co(NO <sub>3</sub> ) <sub>2</sub> x6H <sub>2</sub> O	electrolysis	1005
Cu <sup>2+</sup>	Cu(NO <sub>3</sub> ) <sub>2</sub> x3H <sub>2</sub> O	electrolysis	996
Mn <sup>2+</sup>	Mn(NO <sub>3</sub> ) <sub>2</sub> x4H <sub>2</sub> O	titration with EDTA	997
Fe <sup>3+</sup>	Fe	-	1000
Al <sup>3+</sup>	Al <sub>2</sub> (SO <sub>4</sub> ) <sub>3</sub> x16H <sub>2</sub> O	-	1000
NH <sub>4</sub> <sup>+</sup>	NH <sub>4</sub> Cl	-	1000
Li <sup>+</sup>	Li <sub>2</sub> SO <sub>4</sub>	-	1000
K <sup>+</sup>	KCl	-	1000
Na <sup>+</sup>	NaCl	-	1000
Sr <sup>2+</sup>	SrCl <sub>2</sub> x6H <sub>2</sub> O	comparison by ICP	1000
	Sr(NO <sub>3</sub> ) <sub>2</sub>		1000
Ba <sup>2+</sup>	Ba(NO <sub>3</sub> ) <sub>2</sub>	-	995
Ag <sup>+</sup>	AgNO <sub>3</sub>	potentiometric titrn. with Br <sup>-</sup>	1005 /31/
SO <sub>4</sub> <sup>2-</sup>	K <sub>2</sub> SO <sub>4</sub>	-	1000
NO <sub>3</sub> <sup>-</sup>	KNO <sub>3</sub>	-	1000
PO <sub>4</sub> <sup>3-</sup>	KH <sub>2</sub> PO <sub>4</sub>	-	1000
BO <sub>3</sub> <sup>3-</sup>	H <sub>3</sub> BO <sub>3</sub>	-	1000
Mo <sup>6+</sup>	MoO <sub>3</sub>	-	1000
Mg <sup>2+</sup>	Mg(NO <sub>3</sub> ) <sub>2</sub> x6H <sub>2</sub> O	-	1000
Ca <sup>2+</sup>	Ca(NO <sub>3</sub> ) <sub>2</sub> x4H <sub>2</sub> O	-	1000



## 2.4 Chemical analysis

### 2.4.1 Atomic absorption spectrophotometry

Two different spectrophotometers were used: a Southern Analytical A3000 and Perkin-Elmer 5000. The cations to be determined and their used absorption wavelengths, detection limits and disturbances are listed in Table IV. Hollow cathode lamps and air-acetylene were used /32/.

Table IV. Cations and their used absorption wavelengths. Disturbances and detection limits.

Element	Disturbing compounds or elements	Wavelength	Reached detection limits (mg/dm <sup>3</sup> )
chromium	Fe, Ni	357.87	0.03
manganese	Si *	279.48	0.012
zinc		213.86	0.007
copper	mineral acids *	324.75	0.013
cadmium		228.80	0.01
nickel		232.00	0.04
cobolt	Fe *	240.24	0.05
mercury		253.65	
lead	Ar	217.00	0.08

\* Slightly

The disturbances were eliminated by using standards containing acids and several elements in concentrations corresponding to those in dissolved sample solutions. The accuracy of determinations was about  $\pm 3$  %. The standard addition method was also used.  $\text{NH}_4\text{Cl}$  was added to solutions when chromium was determined.

### 2.4.2 Induction-coupled plasma emission spectrometry

The apparatus used was the Perkin-Elmer 5000. Lines and conditions used are collected in Table V.

The results were confirmed by standard addition method, by using a graphical program made by Perkin-Elmer for the investigation of spectral disturbances, and by using background correction.

Table V. The used lines in induction-coupled plasma analysis.

---

Element	Line (nm)	Notes
Cu	324.75	AAS
Mn	257.61	AAS
Zn	213.86	AAS
Co	228.62	AAS
Ni	231.60	AAS
Cr	205.55	
Al	308.22	
Fe	259.94	
Mg	279.94	AAS
Ca	317.93	
Sr	407.77	
Ba	455.40	
B	249.77	
S	182.04	N <sub>2</sub> -atmosphere
P	213.62	
Mo	281.62	

Code: AAS = precision and sensitivity about equal to that of atomic absorption spectrophotometry

---

Multi-element analysis was used with care, because with some elements the flow rate of argon influences the sensitivity. The flow rate slowly increases during long analysis periods. The accuracy of determinations was about  $\pm 3\%$ .

#### 2.4.3 Infrared spectrometry

The dried (103 °C, 24 h) and milled samples were mixed with dried KBr in a ball mill in the ratio of 1:200. The mixture was pelletized for the run. The IR-spectrometer was a Perkin-Elmer 283 and scanning was performed between wave-number values 4000 and 200  $\text{cm}^{-1}$ .

#### 2.4.4 Flame photometry

Lithium, sodium and potassium were determined by flame photometry (type: EEL). The flame was maintained by propane-butane-air mixture. The colour of the flame was adjusted to blue with air. A special filter for each metal was used. The accuracy was about  $\pm 3 \%$ .

#### 2.4.5 Titrimetric methods

Titrimetric methods were used for silver and  $\text{NO}_3^-$ . Silver was titrated potentiometrically with  $\text{Br}^-$  /31/ and  $\text{NO}_3^-$  was determined by ion selective electrode (type: Orion research). The accuracy was about  $\pm 4 \%$ .

#### 2.4.6 Spectrophotometric methods

Spectrophotometric methods were used for  $\text{Al}^{3+}$ ,  $\text{Fe}^{3+}$ ,  $\text{NH}_4^+$  and  $\text{PO}_4^{3-}$ . The apparatus was a Pye Unicam spectrophotometer. Reagents were aluminon for  $\text{Al}^{3+}$  /33/, 1.10 phenanthroline for  $\text{Fe}^{3+}$  /34/ and Nessler for  $\text{NH}_4^+$  /35/.  $\text{PO}_4^{3-}$  was determined by heteropoly blue method /36/. The accuracy was about  $\pm 4 \%$ .

#### 2.4.7 Thermogravimetry

A dried and milled sample of 10 mg was taken for each run. The flow rate of the gases (mixed gas 20 %  $\text{O}_2$  in  $\text{N}_2$ , or 99.99 %  $\text{N}_2$ ) was 0.0022  $\text{dm}^3 \text{ s}^{-1}$  and heating rate 0.167 °C  $\text{s}^{-1}$ . The thermobalance was a Fischer TGA-system Series 100. The open sample cup was made of platin.

## 2.5 Methods for determining ion exchange capacities

### 2.5.1 Dynamic method

In dynamic experiments the test ion solution was allowed to flow through a peat layer 0.050 m in height. The layer was placed at the bottom of a chromatographic column of length 0.50 m. The peat was carefully moistened in the column and air bubbles were removed by suction before the experiment.

The flow rate was adjusted to a stable value immediately after pouring the test solution into the column. The height of the solution was maintained 25 - 35 cm above the peat surface. The stabilized flow rate was  $0.025 \text{ cm}^3/\text{s}$  measured manually with a stopwatch and the effluent was collected in  $25\text{-cm}^3$  aliquots for analysis. The temperature was  $21 \pm 1 \text{ }^\circ\text{C}$  during experiments and the number of aliquots taken during one experiment was 8 - 16, which is enough for drawing accurate adsorption curves. The curves for calculations were combinations of curves from two or three parallel experiments. The reproducibility was normally  $\pm 5 \%$ , calculated from the capacity values obtained from separate experiments. Figure 8 shows the experimental apparatus.

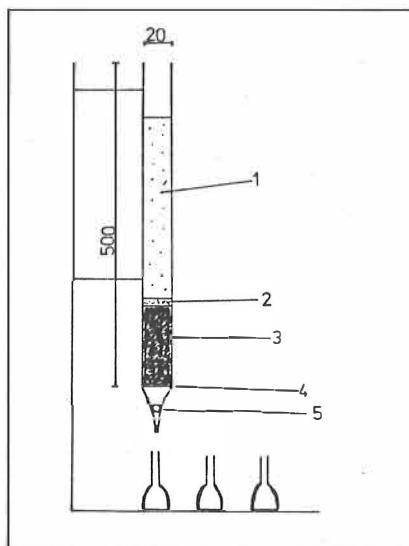


Figure 8. The apparatus used: 1. test solution, 2. glass wool plug, 3. peat with air bubbles removed, 4. ceramic porcelain, 5. precision stopcock.

### 2.5.2 The properties of dynamical adsorption curves

The shape of a typical adsorption curve is shown in Figure 9.

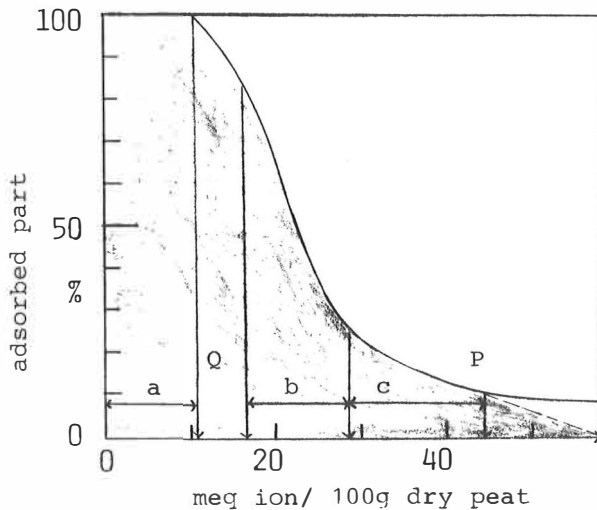


Figure 9. Typical adsorption curve. X-axis: the amount of ions passed through the peat layer. Y-axis: the corresponding adsorbed fraction of the ions.

The adsorption curve can be divided into five regions: the first region with adsorption percentage  $> 99.5$  (a), the second region with high adsorption percentage but irregular behaviour (Q), the descending region, the slope of which obeys the first order kinetic equation (b), the descending region with weak adsorption (c), and the long tail after point P that is extrapolated to zero because of the uncertain and low nature of adsorption. The shaded area between the axis and the curve corresponds to the ion exchange capacity under the conditions used. The width of the high adsorption region  $> 99.5$  % and the slope of the descending region characterize the adsorption behaviour.

### 2.5.3 Calculations from dynamical adsorption curves

Three computer programs were used for calculations. The computer was an ABC-80-type desk computer.

The program "Turvecap" calculated the stepwise adsorption curve. The program consisted of two subprograms: a) Calculation of the concentrations in the eluent fractions collected. Sensitivity changes in a single-beam atomic adsorption spectrophotometer (the most commonly used apparatus) were taken into account /37/. b) Calculation of the stepwise adsorption curve: adsorbance as a function of the amount of ions passed through the peat layer. It was assumed that the moistening water in the peat layer passes out first. According to tests with anions of zero adsorbance, the assumption was approximately correct.

The adsorption curves from two or three identical experiments were combined manually, after calculation with the program "Turvecap".

The program "Turvecomp" calculated the capacity by integration method and followed the shape of the descending region of the curve by calculating the values of  $K_{Comp}$  according to the equation:

$$K_{Comp} = \frac{M \times L}{\bar{M}} \quad (14)$$

where

M = concentration of free cation in the solution (meq/dm<sup>3</sup>)

$\bar{M}$  = concentration of bound cation (meq/100 g peat)

L = concentration of free adsorption places in the sample (meq/100 g) (calculated capacity minus amount adsorbed at a given time)

Program "Turvekin" calculated the degree of fit between the descending part of the curve and the first order kinetic equation:

$$\log (a-x) = - \frac{K}{2.3} t + C \quad (15)$$

where

a = initial concentration (meq/dm<sup>3</sup>)

x = reduction in concentration at the time t (meq/dm<sup>3</sup>)

K = reaction rate constant

t = time (s)

C = constant

#### 2.5.4 Static method

Peat samples were shaken 24 h with the ion solution. The adsorption of the ion was calculated from the reduction in the concentration of that ion in the solution.

Sample amounts and test solutions were alike when shaking static and dynamic experiments were being compared.

### 3 RESULTS AND DISCUSSION

The results from chemical analysis are discussed by sample groups as defined in section 2.1. The samples in group 4 were not analyzed chemically because the purpose there was to study the relevance of production area for the adsorption properties. IR spectrometry was used to study the effect of extraction on the samples in group 5. The samples in groups 1 - 4 were in natural state when adsorption experiments were carried out.

#### 3.1 Elemental analysis

##### 3.1.1 Sample groups 1 and 2

The element contents are listed in Table VI. The amounts of cations indicate the situation in occupied carboxyl groups.

The sample from Rastunsuo contained much more iron, calcium, aluminium and phosphorus than the sample from Haukineva.

##### 3.1.2 Sample group 3

The element contents most interesting from the point of view of the adsorption study are listed in Table VII.

S. Cuspidata H1-2 (in von Post's scale) contained a high potassium content and a moderate iron content. S. Cuspidata H3 peat contained less minerals than the H1-2 sample. S. Fuscum H2 peat contained low concentrations of all elements measured. S. Fuscum H3 peat contained 0.45 % iron, which may decrease its adsorption capacity. The concentrations of all measured elements were comparatively high in S. Palustris H1-2 peat.



Table VI. Element contents in the samples

Sample	(ICP)					
	C %	H %	N %	S %	O %	Inorganic %
A	46.5	5.72	0.76	0.28	43.2	2.5
B	52.8	5.84	2.00	0.42	33.0	5.5

Sample	Method	Cu 2	Mn 2	Zn 2	Co 2	Ni 2	Cl 2	Pb 2	Al 2	Cr 2	Fe 2	Mg 1	Ca 1	Sr 1	Ba 1	Li 1	Na 2	K 2	P 1	Mo 1	B 1
A	AAS	3	67	37	6	3	<0.5	10	-	-	1070	710	1620	-	-	-	-	-	330	3	<0.5
A	ICP	8	66	42	-	-	-	-	420	2	1250	700	1640	5	12	-	-	-	-	-	-
A	FPH	-	-	-	-	-	-	-	-	-	-	-	-	-	7	99	318	-	-	-	
B	AAS	4	71	10	5	6	<0.5	6	-	-	8100	850	3750	-	-	-	-	-	-	-	
B	ICP	9	85	14	-	-	-	-	2000	3	7550	830	3800	25	40	-	-	-	580	<0.5	<1
B	FPH	-	-	-	-	-	-	-	-	-	-	-	-	-	10	98	153	-	-	-	

Concentrations as mg/kg dry peat

AAS = atomic absorption spectrophotometry, average values from three measurements

ICP = induction-coupled plasma emission spectrometry, values from standard addition method

FPH = flame photometry

A = low-moor peat from Haukineva production area H1-2 in von Post's scale

B = medium-moor peat from Rastunsuo production area H5-6 in von Post's scale

1 = after  $\text{HNO}_3$  -  $\text{HClO}_4$  4:1 wet combustion

2 = after  $\text{HF}$  -  $\text{HNO}_3$  -  $\text{CH}_2\text{O}_4$  6:4:1 wet combustion

C, H, N and O were determined at the Finnish Pulp and Paper Research Institute, Espoo.

Table VII. Major element contents and concentrations of the most important cations /38, 39/.

Sample	H*	Code	µg/g dry peat							Percentage		
			K (A,2)	Ca (B,1)	Sr (B,1)	Mn (C,2)	Fe (D,2)	Cu (C,2)	Zn (C,2)	H	C	N
<u>S. Cuspidata</u>	1-2	1	4730	1060	6.3	56	1480	41	79	6.0	44.5	1.09
"	3	2	1270	806	7.5	56	740	13	33	6.2	47.1	1.07
<u>S. Fuscum</u>	2	3	340	1240	4.5	34	610	10	24	6.0	46.0	0.39
"	3	4	170	1530	5.8	29	4530	4	25	5.9	45.9	0.42
<u>S. Palustria</u>	1-3	5	2960	1950	12.3	80	2320	33	71	6.0	45.5	0.71

(A) = by flame photometry

(B) = by induction-coupled plasma emission spectrometry

(C) = by atomic absorption spectrophotometry

(D) = by colorimetric method

H\* = degree of humification by von Post

(1) = after HNO<sub>3</sub> - HClO<sub>4</sub> 4:1 wet combustion

(2) = after HF - HNO<sub>3</sub> - HClO<sub>4</sub> 6:4:1 wet combustion

Code	mg/g dry peat	
	S (B,1)	P (B,1)
1	3400	390
2	2300	150
3	1100	80
4	1100	220
5	1800	160

### 3.2 Infrared spectrometry

The most significant IR-absorption areas can be found at wavenumber regions  $1600 - 1750 \text{ cm}^{-1}$  and  $1000 - 1200 \text{ cm}^{-1}$ . The free carboxyl groups absorb at  $1708 - 1727 \text{ cm}^{-1}$ . These groups are able to bind metal ions, and the absorption at  $1600 - 1650 \text{ cm}^{-1}$  is due to the bound carboxyl groups. The range  $1030 - 1085 \text{ cm}^{-1}$  is important since alcohol and polysaccharide functional groups, which may also bind metal ions, absorb in this range [40, 41]. Other groups that can easily be seen in the IR spectra of peat are hydroxyl (broad signal at about  $3400 \text{ cm}^{-1}$ ), aliphatic hydrocarbon ( $2920$  and  $2850 \text{ cm}^{-1}$ ) and aromatic ring ( $1610$  and  $1510 \text{ cm}^{-1}$ ) groups (Figure 10).

#### 3.2.1 Sample groups 1 and 2

Figure 10 shows the important regions in the IR spectra of dried and copper-saturated samples (at pH 3.0, column experiment).

The sample A (from Haukineva) had a higher concentration of  $\text{COO}^-$ -groups than sample B (from Rastunsuo), as can be estimated from the total area of the two  $\text{COO}^-$  peaks. The ratio of free groups ( $1720 \text{ cm}^{-1}$ ) to occupied groups ( $1620 \text{ cm}^{-1}$ ) is not easy to estimate, because the two signals overlap. Sample A contained more alcohols and polysaccharides than sample B. The adsorption of Cu has no great influence on the spectra because the amount of the cation adsorbed is small relative to the amount of  $\text{COO}^-$  groups.

The influence of benzol-ethanol extraction in soxhlet apparatus on the  $-\text{CH}_2-$ ,  $\text{CH}_3-$  signals at  $2920 - 2850 \text{ cm}^{-1}$  was studied, and Figure 11 shows the results, where the spectra of the untreated and extracted samples are plotted for the region  $2500 - 4000 \text{ cm}^{-1}$ . In addition, the Figure shows the spectra of the fractions recovered after drying of the extraction mixture.

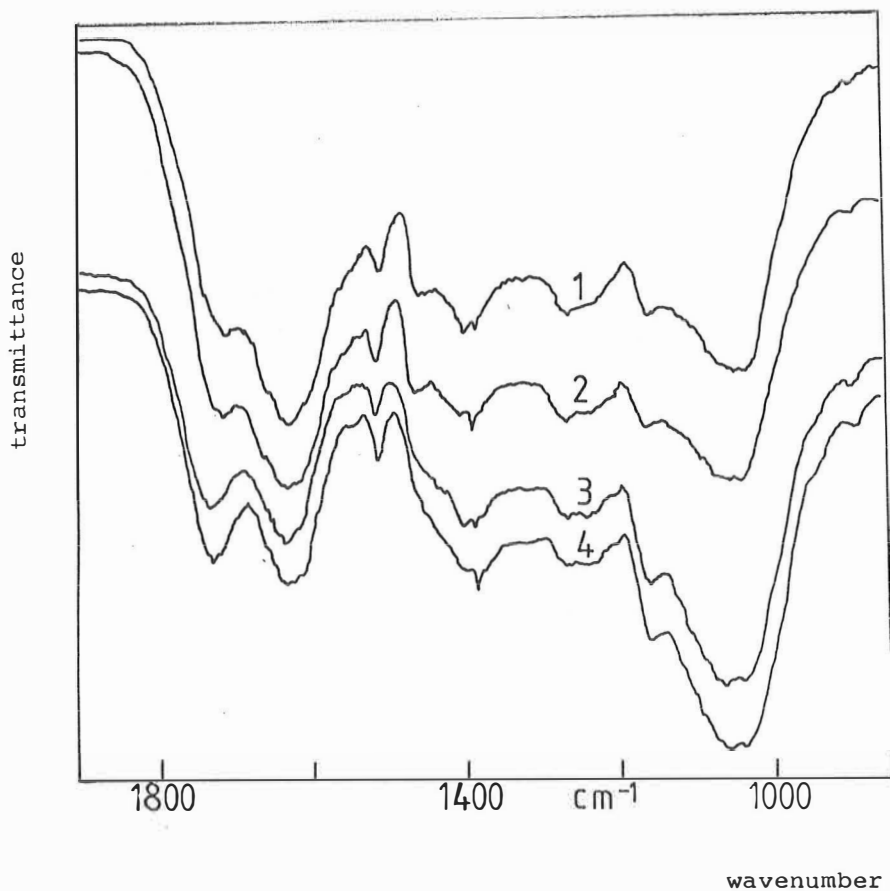


Figure 10. Parts of the IR spectra of the samples under study. 1 = sample B, 2 = sample B saturated with copper ions at pH 3.0 3 = sample A, 4 = sample A saturated with copper ions at pH 3.0.

The extraction had a clearly stronger effect on the spectrum of the peat from Rastunsuo. The low-moor sample contained much less long-chain hydrocarbons and correspondingly the effect on the spectrum was smaller. The hydrocarbon signals of the extracted fractions confirmed the expected result.

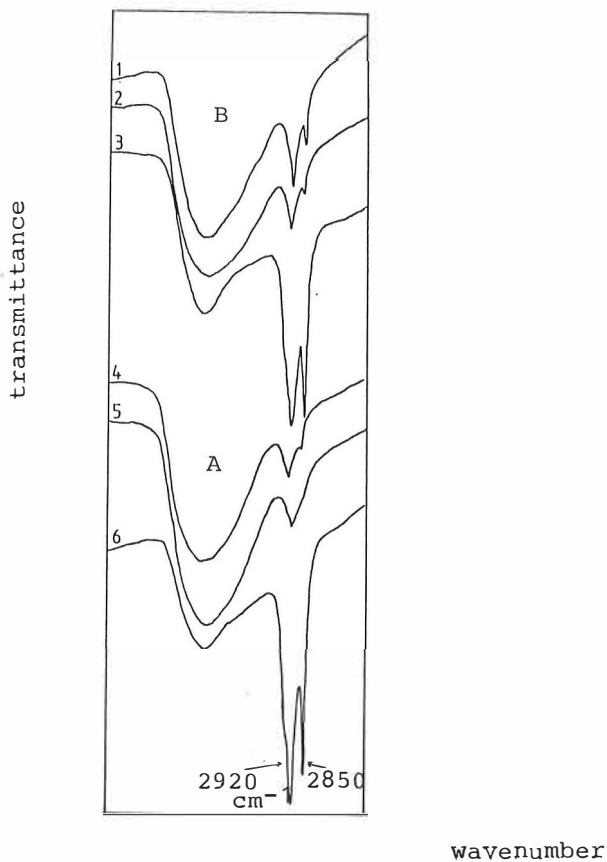


Figure 11. The IR spectra obtained from extraction experiments. B1 = Untreated peat H5-6 from Rastunsuo, B2 = after extraction, B3 = extracted fraction, B4 = untreated peat H1-2 from Haukineva, B5 = after extraction, B6 = extracted fraction.

### 3.2.2 Sample group 3

Figure 12 shows the important region of the IR spectra of the samples.

The ratio of free carboxyl groups ( $\sim 1720 \text{ cm}^{-1}$ ) to occupied groups ( $\sim 1620 \text{ cm}^{-1}$ ) is difficult to determine precisely. S. Fuscum peats and especially S. Fuscum H2 tended to have a high concentration of free  $\text{COO}^-$  groups.

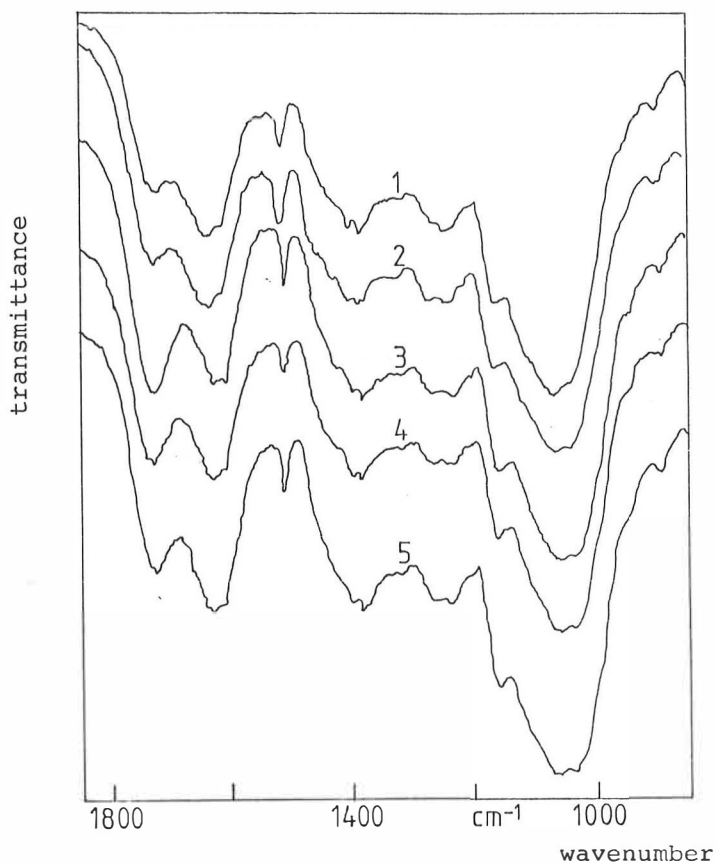


Figure 12. The important parts of the IR spectra of the Sphagnum peats studied. 1 = S. Cuspidata H1-2, 2 = S. Cuspidata H 3, 3 = S. Fuscum H2, 4 = S. Fuscum H3, 5 = S. Palustria H1-2.

### 3.3 Thermogravimetry

Thermogravimetry was used to estimate roughly the relative amounts of cellulose, hemicellulose and lignin-based compounds in peat. The low initial temperature of the reactions shows the existence of easily reactive hemi-cellulosic compounds. The high weight loss in nitrogen shows the high content of celluloses and hemicelluloses and corresponds to low degree of humification. The amount of residue in mixed gas shows the mineral content.

### 3.3.1 Calculations

The first stage was to digitalize the region of the weight curve representing a particular reaction to 7-9 points with weight value and corresponding temperature. From these points the program calculated the activation energy, frequency factor and reaction order according to methods published by Broido /42/ and Coats and Redfern /43/.

The calculation methods are illustrated as follows /44/:

If the pyrolysis is carried out in an isothermal way, the velocity of the reaction obeys the equation

$$\frac{d\alpha}{dt} = k(T)f(\alpha) \quad (16)$$

where

$k(t)$  = specific rate constant

$\alpha$  = mole fraction of the decomposed material at the moment  $t$

Let us define

$$f(\alpha) = (1 - \alpha)^n \quad (17)$$

where

$n$  = the order of the reaction

and

$$k(T) = Ae^{-E^*/RT} \quad (18)$$

If the pyrolysis is carried out non-isothermally, Eqs. (16), (17) and (18) give

$$\frac{d\alpha}{(1 - \alpha)^n} = \frac{A}{u} e^{-E^*/RT} dT \quad (19)$$

where

$u$  = the linear heating rate  $Ks^{-1}$

Integration of Eq (19) gives

$$F(\alpha) = \int_{\alpha_0}^{\alpha} \frac{d\alpha}{(1 - \alpha)^n} = \frac{A}{u} \int_{T_0}^T e^{-E^*/RT} dT = G(T, E^*, A/u) \quad (20)$$

The integral on the left-hand side takes the form

$$F(\alpha) = \ln [1/(1 - \alpha)] \quad (21)$$

when  $n = 1$  and  $4$ , and

$$F(\alpha) = \frac{1 - (1 - \alpha)^{1-n}}{1 - n} \quad (22)$$

when  $0 < n < 1$

Several different approximations have been proposed for the integral on the right-hand side. The following are perhaps most often applied.

After taking logarithms in Eq. (20) Broido used the approximation

$$\ln F(\alpha) \approx -(E^*/R) (1/T) + \text{constant} \quad (23)$$

Coats and Redfern introduced the approximation

$$G(T, E^*, A/u) \approx \frac{ART^2}{uE^*} \left[ 1 - \frac{2RT}{E^*} \right] e^{-E^*/RT} \quad (24)$$

and after taking logarithms obtained

$$\log \left[ \frac{F(\alpha)}{T^2} \right] = -\frac{E^*}{2.3 RT} + \log \left[ \frac{AR}{uE^*} \left( 1 - \frac{2RT}{E^*} \right) \right] \quad (25)$$

Balarin has presented the exact integral

$$G(T, E^*, A/u) = \frac{ART^2}{uE^*} e^{-E^*/RT} \times \eta(\gamma) \quad (26)$$



where

$$\eta(y) = 1 - \sum_{i=1}^k (-1)^{i+1} (i+1)! y^i,$$

$$y = \frac{RT}{E^*}$$

$$k = \left(\frac{1}{\lambda y} - 2\right)$$

The logarithm of the exact integral of Eq. (26) can be written, following Broido, as

$$\ln F(\alpha) = \frac{1}{\lambda y} + \ln \left[ \frac{AyT}{u} \eta(y) \right] \quad (27)$$

or use can be made of the Coats-Redfern manipulation, giving

$$\log \left[ \frac{F(\alpha)}{T^2} \right] = - \frac{1}{2.3y} + \log \left[ \frac{Ay}{uT} \eta(y) \right] \quad (28)$$

The Eqs. (23), (25), (27) and (28) become linear when  $X = 1/T$  and the left-hand side of the equations is  $Y$ .

The linear equation can be solved with the help of the least-squares method. After finding the value of  $n$  with respect to  $F(\alpha)$  on the basis of the best regression coefficient, the slope of the corresponding linear equation gives the value of  $E^*$  and the intersection gives the value of  $A$  according to Eqs. (25), (27) and (28). Equation (18) was used to evaluate  $k(T)$ .

### 3.3.2 Sample groups 1 and 2

Figure 13 shows the thermogravimetric (TG) curves of the samples in nitrogen, and Figure 14 shows the corresponding curves in mixed gas (80 %  $N_2$ , 20 %  $O_2$ ).

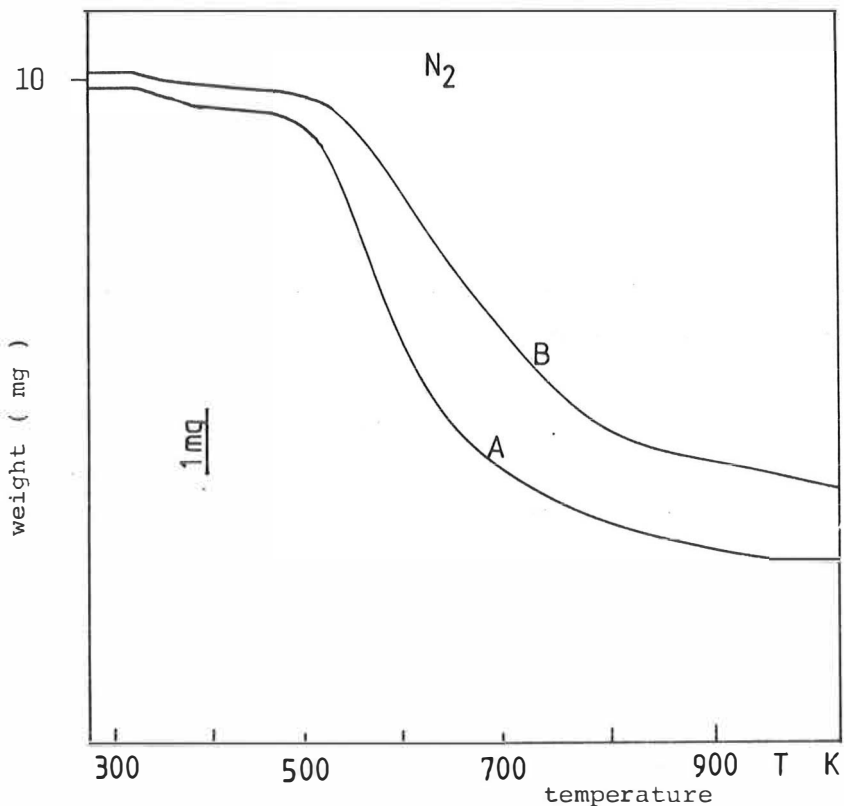


Figure 13. The TG-curves of the peat samples in nitrogen. Codes as in Table VIII.

The curves have different shapes in air and in nitrogen. Sample A contains more volatiles: about 74 %. Sample B contains about 65 %. That corresponds to the lower degree of humification of sample A and its higher content of hemicellulose and cellulose. The parameters calculated from TG curves are collected in Table VIII.

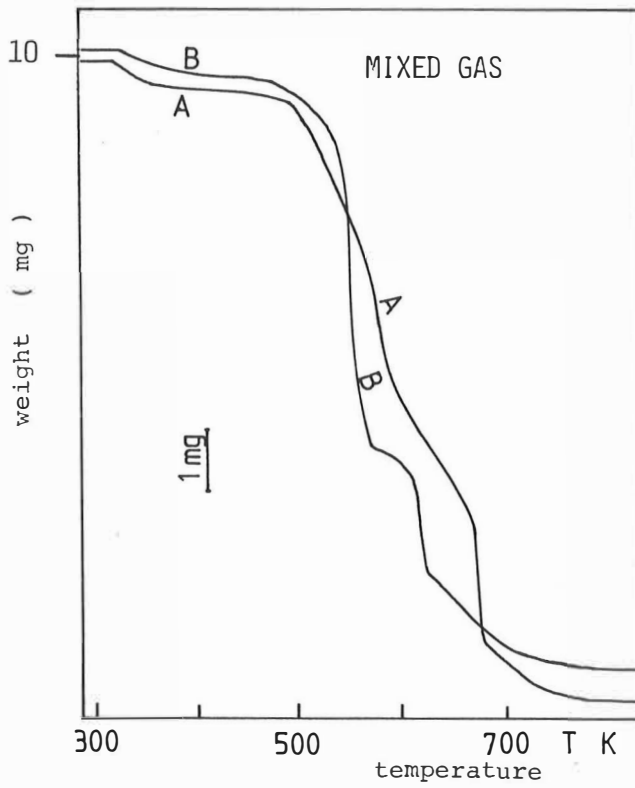


Figure 14. The TG curves of the peat samples in mixed gas.  
Codes as in Table VIII.

Table VIII. Kinetic parameters calculated from thermogravimetric curves. Calculation methods: Broido and Coats-Redfern.

Sample	Reaction	Atmosphere	$\Delta W_{abs}$	$T_{init}$	$T_{fin}$	n	E	logA	-R	n	E	logA	-R
						B	B	B	B	C	C	C	C
A	1	mixed	47.5	459	562	0.99	102	7.83	0.994	0.99	93.5	6.96	0.993
A	2	"	68.5	627	667	0.53	354	26.2	0.994	0.30	326	23.9	0.996
A	1	N <sub>2</sub>	49.7	452	636	0.99	79.9	5.03	0.992	0.99	71.7	4.14	0.990
B	1	mixed	57.5	457	564	0.22	103	7.55	0.998	0.30	96.0	6.86	0.998
B	2	"	43.3	585	620	0.27	315	24.9	0.979	0.04	293	22.9	0.988
B	1	N <sub>2</sub>	49.8	481	731	1.00	63.3	2.78	0.972	1.00	53.5	1.50	0.959

Codes in table:

A = Sample H1-2 from Haukineva production area  
 B = Sample H5-6 from Rastunsuo production area  
 $\Delta W_{abs}$  = Weight loss per cent in the reaction studied %  
 $T_{init}$  = Initial temperature in the reaction K  
 $T_{fin}$  = Final temperature in the reaction K  
 n = Reaction order  
 E = Activation energy kJ/mole  
 A = Frequency factor 1/s  
 C = By Coats-Redfern method  
 B = By Broido method  
 R = Regression coefficient  
 mixed = 20 % O<sub>2</sub> in N<sub>2</sub>

### 3.3.3 Sample group 3

The thermogravimetric curves of the samples are presented in Figure 15.

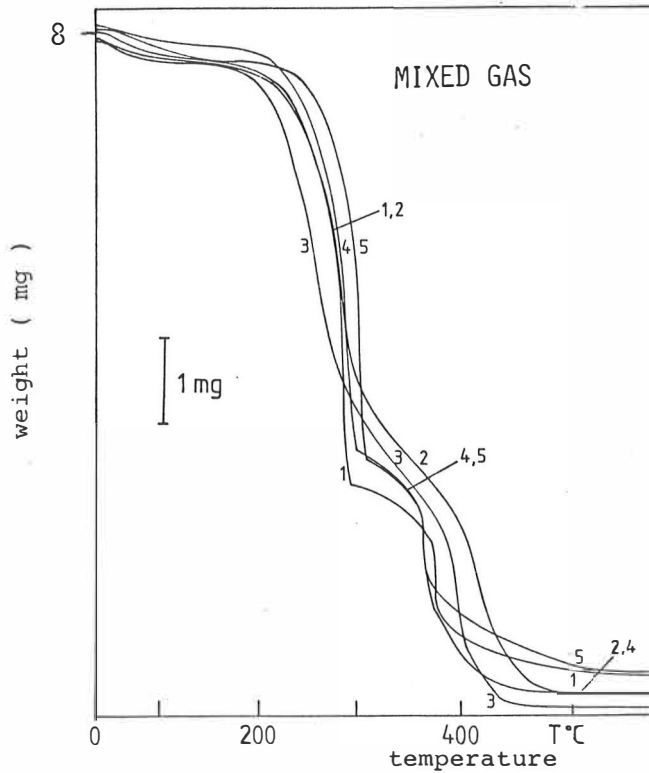


Figure 15. The thermogravimetric curves of the samples recorded in mixed gas (20 % O<sub>2</sub>, 80 % N<sub>2</sub>). Codes as in table VIII.

The experiments performed in mixed gas reveal differences between the samples. S. Cuspidata H1-2 and S. Palustris H1-2 contained more inorganic matter than the other samples. S. Fuscum H2 had lowest mineral content. The order of mineral contents corresponds roughly to the sum of K, Ca and Fe amounts calculated on the basis of Table VII. The parameters calculated from TG curves are collected in Table IX. The samples 1, 4 and 5 had greater  $\Delta W$  value (mass loss

Table IX. The thermogravimetric parameters of the samples.

Sample	Code	T <sub>init</sub> K	T <sub>fin</sub> K	ΔW	Method B			Method C		
					E*	logA	R	E*	log A	R
<u>S. Cuspidata</u>	1	440	569	65	92	6.4	1.000	82	5.4	1.000
"	2	459	573	50	103	7.5	1.000	94	6.6	1.000
<u>S. Fuscum</u>	3	437	553	44	105	8.2	0.997	99	7.6	0.999
"	4	447	571	61	99	7.2	0.995	92	6.4	0.995
<u>S. Palustria</u>	5	462	573	62	117	8.8	0.996	107	7.9	0.997

Codes as in Table VIII.

percent in reaction step) than samples 2 and 3. The  $\Delta W$  value corresponds to the amount of easily reactive compounds. The hemicellulose content in sample 3 is probably higher than that in sample 4 because sample 3 has lower initial temperature in its reaction.

### 3.4 Adsorption properties

#### 3.4.1 The effects of experimental conditions on adsorption in column experiments

To ensure that the tendencies observed were representative, the experiments were performed using two peats of different ion exchange capacity (group 1). The low-moor peat sample H1-2 (from Haukineva) code A had about two times higher capacity at pH 3.0 than the medium-moor peat sample H5-6 (from Rastunsuo) code B. The cation used in tests was  $\text{Cu}^{2+}$  /45/.

The parameters studied in ion exchange experiments were pH and concentration of the test solution, height of the column and flow rate.

If not varied the parameters were as follows: flow rate  $0.025 \text{ cm}^3/\text{s}$ , column height 5.0 cm, concentration of the test solution  $100 \text{ mg}/\text{dm}^3$  and pH 3.0.

##### 3.4.1.1 The mechanism of ion exchange

The mechanism of the ion exchange was studied by following the amount of released  $\text{H}^+$ -ions as a function of the amount of adsorbed copper at initial pH value of 4.9. (Apparatus: Orion pHm). The results can be seen in Figure 16.

The samples differed markedly in their ion exchange mechanisms. In sample B the amount of released  $\text{H}_3\text{O}^+$  ions was small and the most important mechanism was neutral ion exchange and complexing. In sample A the reaction was pure proton-copper exchange between 40 and 100 % saturation. In the beginning also neutral ion exchange and complexing took place.

pH=4.9

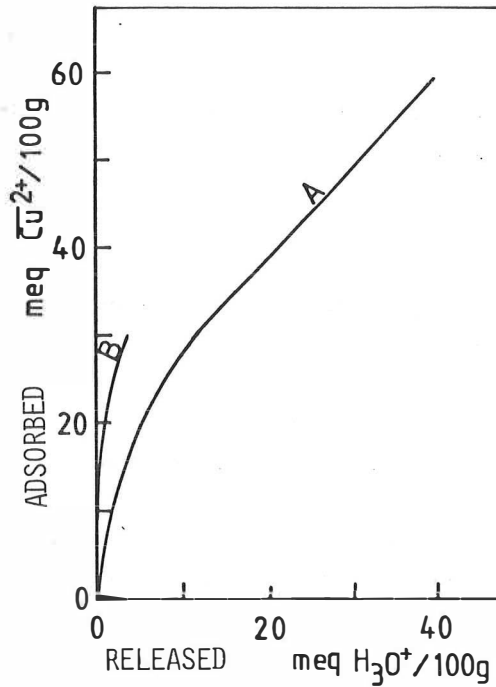


Figure 16. The amount of released hydronium ions as a function of adsorbed copper.

#### 3.4.1.2 Effect of pH

The adsorption curves obtained for solutions with different pH values are shown in Figure 17.

When the pH of the solution is higher than 3.0 there is a high adsorption level at the beginning of the adsorption curve where the adsorption percent is > 99.5 %. The curve then descends in a manner that obeys well the first order kinetic equation (Eq. 15).

The half-life of the reaction can be calculated from the equation

$$t_{\frac{1}{2}} = \frac{2.303 \times \log 2}{K} \quad (29)$$

where

K = kinetic rate constant



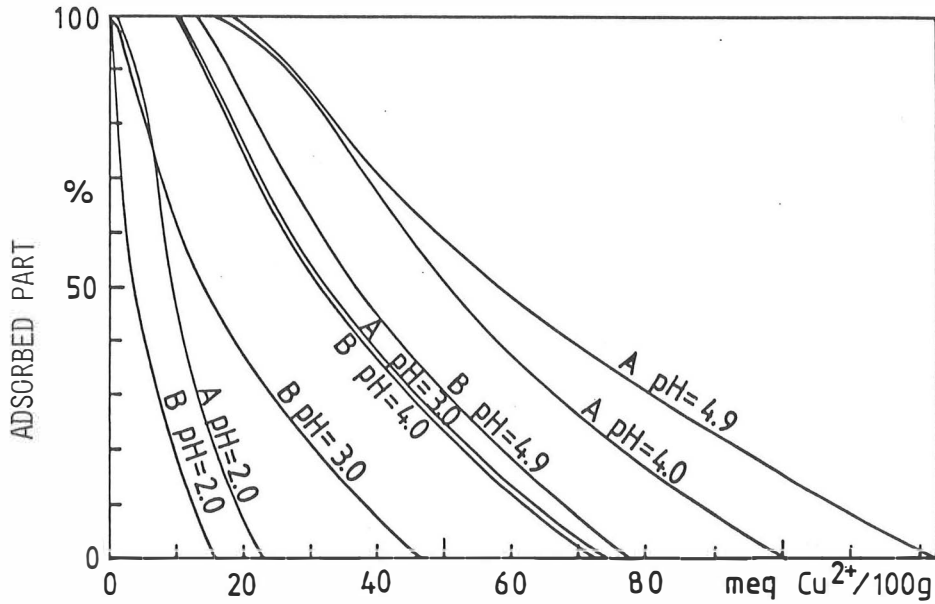


Figure 17. Adsorption curves for different pH values  
A = Haukineva peat, B = Rastunsuo peat,  
C = 100 mg/dm<sup>3</sup>, flow rate = 0.025 cm<sup>3</sup>/s, column  
height 5.0 cm.

The influence of pH on the capacity is seen in Figure 18.

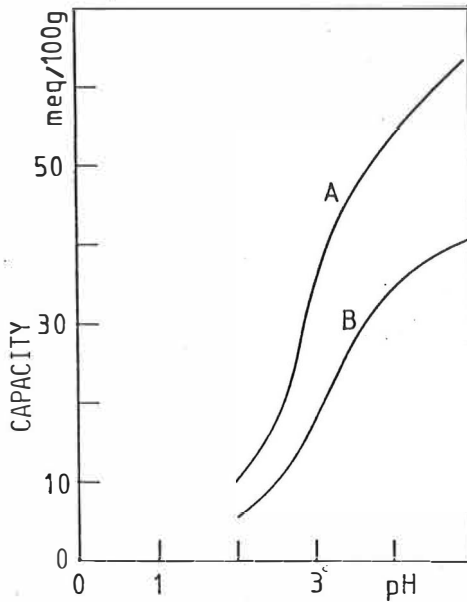


Figure 18. The values of ion exchange capacities as a  
function of pH. The conditions are the same as  
in Figure 17.

Below the pH value  $\sim 1.5$  there is no adsorbance and only releasing of bound cations takes place.

The calculated half-lives (as a function of pH) are plotted in Figure 19. The curves show the relative increase of the values in the conditions studied.

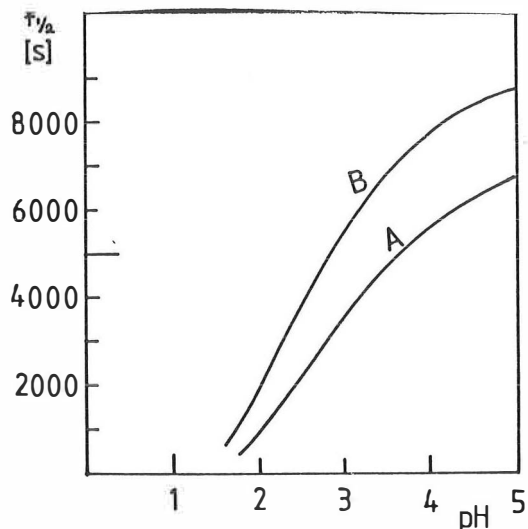


Figure 19. Half-life calculated from the slopes of the curves.

#### 3.4.1.3 Effect of flow rate

The flow rate was varied between 0.025 and 0.1 cm<sup>3</sup>/s (1.5 and 6 cm<sup>3</sup>/min). So the cations had 160 - 420 s time to fix onto the peat layer (volume 16 cm<sup>3</sup>). Figure 20 shows the results.

The flow rate had practically no effect on the capacity in the region studied.

Because the peat samples differ in structure the dry weight of the peat column depends on the peat type. For example sample B was of greater density than sample A, and so the flow rate calculated from the dry weight of the samples was

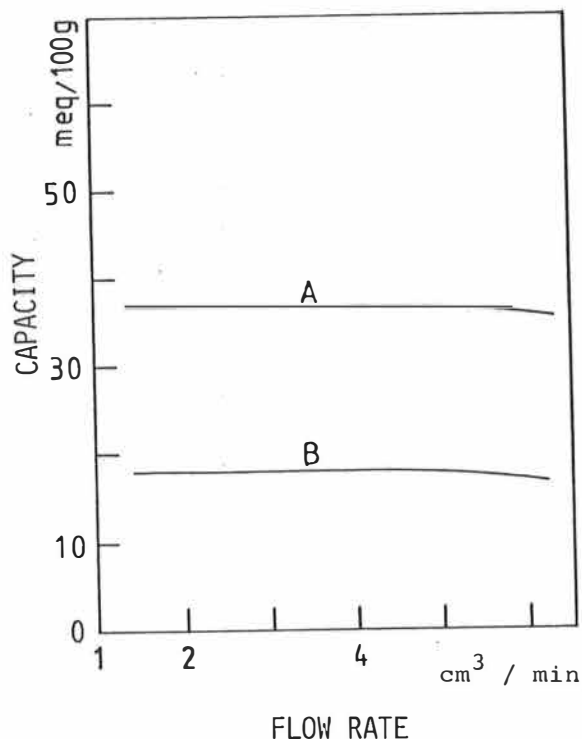


Figure 20. The influence of flow rate on the capacity.  
Column height = 5.0 cm, C = 100 mg/dm<sup>3</sup>.

was greater with sample A. This had no influence on the adsorption curves, however, because the reaction was rapid enough for the ions to reach equilibrium.

#### 3.4.1.4 Effect of concentration

The concentration of the copper solution was varied between 100 and 400 mg/dm<sup>3</sup> (3.2 and 12.8 meq/dm<sup>3</sup>). Figure 21 shows the results.

When the concentration was > 200 mg/dm<sup>3</sup> (> 6.3 meq/dm<sup>3</sup>) there was little effect on the capacity. With values < 100 mg/dm<sup>3</sup> (< 3.2 meq/dm<sup>3</sup>), the effect of concentration was moderate at pH 3.0.

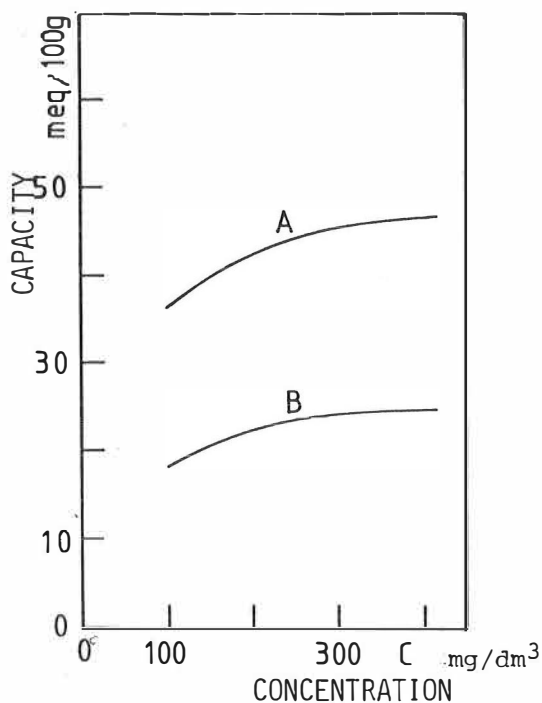


Figure 21. Effect of the concentration of the copper solution on the capacity.

#### 3.4.1.5 Effect of column height

The column height was varied between 1.5 and 5 cm. Figure 22 shows the results.

The height of the column had a slight effect on the capacity and the short columns seemed to be slightly more saturated after the experiment. However, the shape of the adsorption curve was not satisfactory with short columns because the constant region of the curve (adsorption percent > 99.5) was narrow, the curve was tailing and part of the solution flowed easily through passages in the peat layer without ion exchange reaction. A column about 5.0 cm in height is thus more effective.

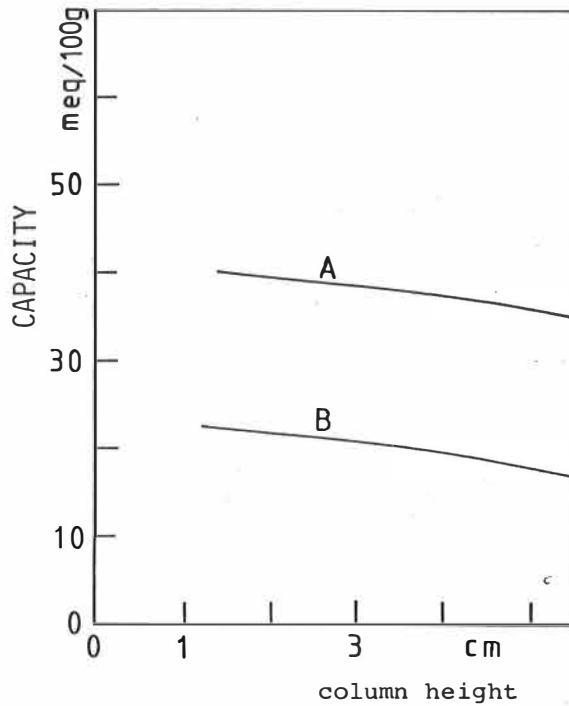


Figure 22. The effect of column height on the capacity.  
Flow rate =  $0.025 \text{ cm}^3/\text{s}$ , pH = 3.0, C =  $100 \text{ mg}/\text{dm}^3$  ( $3.15 \text{ meq}/\text{dm}^3$ ).

#### 3.4.1.6 Summary of the effects

The results from the column experiments with varying parameters are collected in Table X. pH has the strongest influence on adsorption. Solution concentration is of less importance, and flow rate has no effect in the region studied. It is recommended that column height be kept at 5 cm to avoid direct flow through passages in the peat.

The values of  $K_{\text{comp}}$  calculated by equation 14 are not very logical. Column height had practically no effect on the values with sample B, but the effect was moderate with sample A. Increasing pH increased the value of  $K_{\text{comp}}$  with sample A, but there were irregularities with sample B, where the mechanism was far from pure  $\text{Cu}^{2+}$ -proton exchange. In almost every case the value of  $K_{\text{comp}}$  remained within very narrow limits at 55 - 35 adsorption per cent.

Table X. The values of parameters calculated from column experiments

Sample	Column height cm	pH	Concentration meq/dm <sup>3</sup>	Flow rate μeq/100gxs	Capacity meq/100 g	log K <sub>comp</sub> 1	log K <sub>kin</sub> 2	Regression 3	t $\frac{1}{2}$ s
B	5.0	3.0	3.15	2.5	17.7	0.39	-3.89	1.000	5350
B	2.3	3.0	3.15	4.5	22.3	0.36	-3.70	0.998	3470
B	1.2	3.0	3.15	8.7	22.6	0.34	-3.36	1.000	1590
A	5.0	3.0	3.15	4.9	35.9	0.32	-3.76	1.000	3960
A	2.7	3.0	3.15	10.3	39.0	0.55	-3.54	1.000	2440
A	1.4	3.0	3.15	19.5	40.3	0.74	-3.33	0.999	1480
B	5.0	3.0	3.15	4.6	18.1	0.56	-3.69	0.999	3360
B	5.0	3.0	3.15	9.2	16.8	0.48	-3.35	0.999	1570
A	5.0	3.0	3.15	10.0	37.5	0.26	-3.45	1.000	1930
A	5.0	3.0	3.15	20.3	35.7	0.36	-3.16	1.000	1000
B	5.0	3.0	6.30	4.7	22.8	0.40	-3.67	1.000	3200
B	5.0	3.0	12.6	9.2	24.6	0.67	-3.53	0.998	2330
A	5.0	3.0	6.30	9.9	42.7	0.48	-3.51	1.000	2240
A	5.0	3.0	12.6	19.8	46.5	0.75	-3.35	0.998	1550
B	5.0	4.9	3.15	2.3	40.0	0.28	-4.10	1.000	8770
B	5.0	4.0	3.15	2.3	34.8	0.29	-4.06	0.997	7930
B	5.0	2.0	3.15	2.4	5.3	0.00	-3.42	1.000	1830
A	5.0	4.9	3.15	5.0	63.3	0.50	-4.00	0.999	6950
A	5.0	4.0	3.15	5.0	53.8	0.30	-3.83	1.000	4720
A	5.0	2.0	3.15	4.9	10.5	0.22	-3.16	1.000	990

1 = by equation 14    2 = by equation 15    3 = by equation 29

The parameters calculated by Eqs. 15 and 29 represent an important part of the adsorption curves (usually adsorption per cent range 75 - 20 %). The regression coefficients show that the descending parts of the curves obey the first order kinetic equation.

Lalancette /46/ has reported on several dynamical column experiments. The cation studied was  $\text{Hg}^{2+}$ , and a strong effect of pH on the adsorption was found.

#### 3.4.2 The adsorption of representative amounts of ions on medium-moor peat

The adsorption of several ions on medium-moor peat was studied to investigate the adsorption selectivity of peat. Column experiments were emphasized with shaking experiments performed to provide material for comparison. Single ion solutions were used in all experiments. The concentrations of solutions were selected such that a moderate degree of saturation was reached after taking out 8 - 12 fractions of effluent from column experiments. The volume of the solution added in shaking experiments was 200  $\text{cm}^3$  with divalent transition metals and 100  $\text{cm}^3$  with other ions. The amount of peat used in experiments was about 2.6 g dry peat, which was equivalent to about 16  $\text{cm}^3$  moist peat.

##### 3.4.2.1 Results for six divalent transition metals and $\text{Pb}^{2+}$

The concentrations of the solutions of divalent cations tested are listed in Table XI. pH was adjusted with nitric acid.

Table XI. The concentrations in the solutions of divalent transition metals and  $\text{Pb}^{2+}$  used in experiments.

Cation	Mol. wt./charge	Concentration ( $\text{mg}/\text{dm}^3$ )	( $\text{meq}/\text{dm}^3$ )	pH
$\text{Mn}^{2+}$	27.47	50	1.82	3.3
$\text{Ni}^{2+}$	29.35	50	1.70	3.3
$\text{Co}^{2+}$	29.47	50	1.70	3.3
$\text{Zn}^{2+}$	32.69	50	1.53	3.3
$\text{Cd}^{2+}$	56.20	100	1.78	3.3
$\text{Cu}^{2+}$	31.77	100	3.15	3.0
$\text{Pb}^{2+}$	103.6	200	1.93	2.9

According to initial semiquantitative experiments the ion exchange capacity of lead and copper was much higher, in that order, than that of other cations in the table. In order to avoid the analysis of unreasonable amounts of effluent fractions, the pH of Cu and Pb solutions was lowered 0.3 - 0.4 pH units and concentration was higher than in the solutions of other cations.

Figure 23 shows the adsorption curves of cations listed in Table IX.

The efficiencies of column and shaking experiments are compared in Figure 24, where the Y-axis is the capacity (as  $\text{meq}/100$  g dry peat).



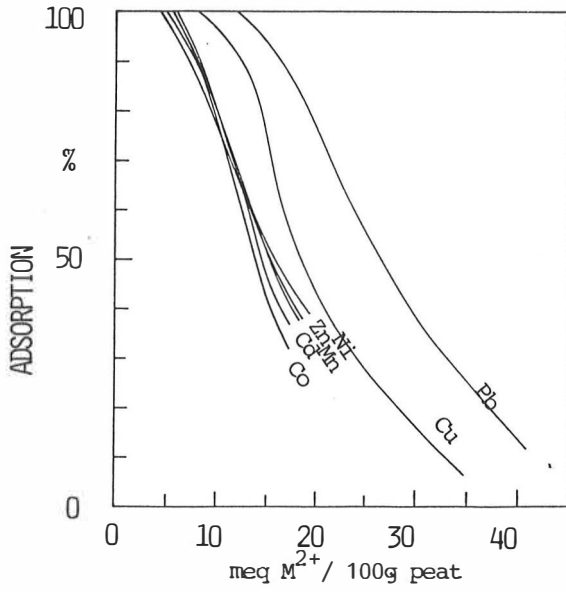


Figure 23. The adsorption curves of single metal ions on the medium-moor peat from Rastunsuo in column experiments.

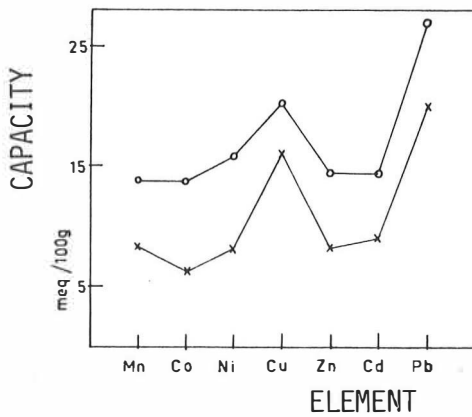


Figure 24. Comparison of the capacities of column (o) and shaking (x) experiments.

The column experiment is more efficient and the adsorption level of > 99.5 % can be reached only by that method in the conditions used. In shaking experiments the major mechanisms are neutral ion exchange and adsorption because the changes in pH are small and the pH value increases slightly during the reaction, as is shown by Figure 25. The major mechanisms are also the same with Rastunsuo peat in column experiments, as can be seen in Figure 16 (sample B) where the cation is  $\text{Cu}^{2+}$  /47/.

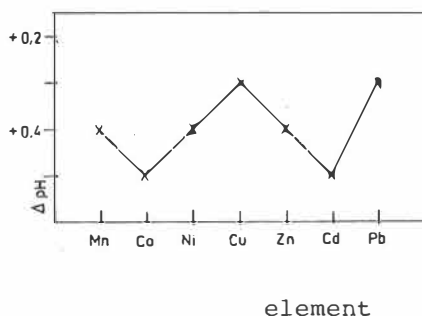


Figure 25. The change in hydronium ion content in the solution during the shaking experiment (shaking time 20 h).

The order of adsorption in column experiments was  $\text{Pb}^{2+} > \text{Cu}^{2+} > \text{Ni}^{2+} > \text{Zn}^{2+} \sim \text{Cd}^{2+} \sim \text{Mn}^{2+} \sim \text{Co}^{2+}$ . The corresponding order in shaking experiments was  $\text{Pb}^{2+} > \text{Cu}^{2+} > \text{Cd}^{2+} > \text{Zn}^{2+} \sim \text{Ni}^{2+} \sim \text{Mn}^{2+} > \text{Co}^{2+}$ . The orders are in conformity with the order found in the complex stability studies performed by Irwing and Williams /48/.

The effect of pH on the adsorption of  $\text{Cd}^{2+}$  on the sample was studied by column experiments and the results are summarized in Figure 26. The effect was similar to that for copper shown in Figures 17 and 18.

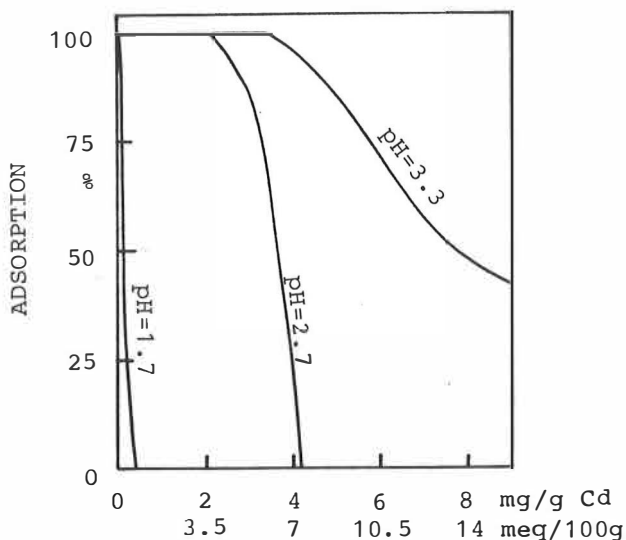


Figure 26. The influence of pH on the adsorption of cadmium in the column experiment.

#### 3.4.2.2 Results for other ions

The concentrations of the solutions were as follows:  $\text{NH}_4^+$  25 mg/dm<sup>3</sup>,  $\text{Li}^+$  50 mg/dm<sup>3</sup>,  $\text{Na}^+$  50 mg/dm<sup>3</sup>,  $\text{K}^+$  50 mg/dm<sup>3</sup>,  $\text{Mg}^{2+}$  50 mg/dm<sup>3</sup>,  $\text{Ca}^{2+}$  50 mg/dm<sup>3</sup>,  $\text{Sr}^{2+}$  250 mg/dm<sup>3</sup>,  $\text{Ba}^{2+}$  50 mg/dm<sup>3</sup>,  $\text{NO}_3^-$  10 mg/dm<sup>3</sup>,  $\text{H}_2\text{PO}_4^-$  10 mg/dm<sup>3</sup> (as N and P). The pH of all the solutions was 3.3 /49/.

Figure 27 shows the adsorption curves of alkalies and alkaline earths.

The most surprising result was the high capacity of peat for strontium. To ensure that there was no mistake, the cation was eluted from the column with 1 mol/dm<sup>3</sup>  $\text{HNO}_3$ . 99 % of the strontium adsorbed on peat was released with 75 cm<sup>3</sup>  $\text{HNO}_3$ . The experiment was then repeated using  $\text{SrCl}_2$  solution instead of  $\text{Sr}(\text{NO}_3)_2$  and the capacity value obtained was the same. These results confirm the great selectivity of peat when solutions are relatively dilute and pH is low.

The adsorption curves of trivalent cations,  $\text{Ag}^+$  and  $\text{Hg}^{2+}$  are shown in Figure 28.

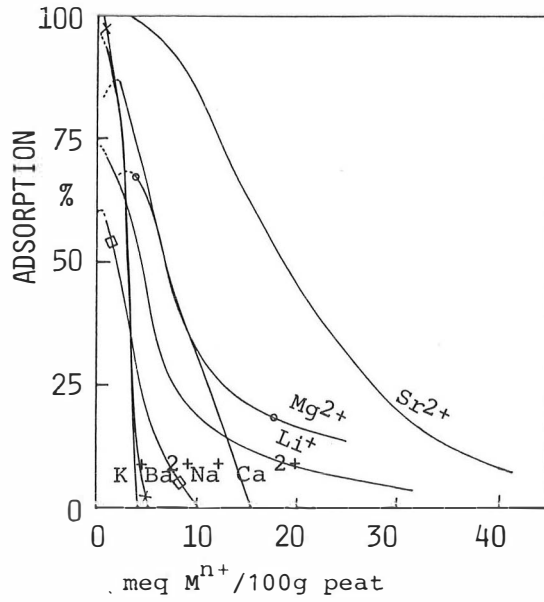


Figure 27. The adsorption curves of alkalis and alkaline earths for peat from Rastunsuo, at pH 3.3.

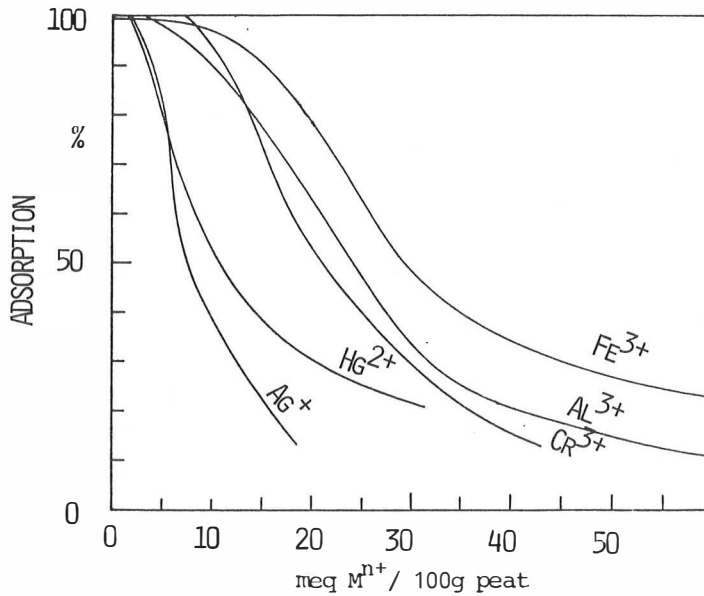


Figure 28. The adsorption curves of some trivalent cations, Ag<sup>+</sup> and Hg<sup>2+</sup> for peat from Rastunsuo, at pH 3.3.

The capacities of column and shaking experiments are compared in Figure 29.

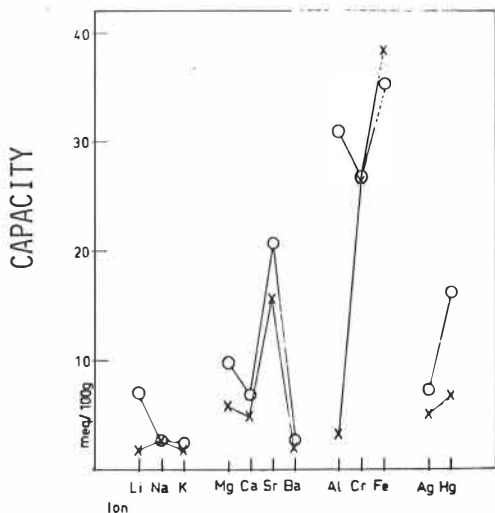


Figure 29. Comparison of the capacities of column (o) and shaking (x) experiments.

The notable feature of Figure 29 is the much stronger adsorption of cations with great surface charge such as  $\text{Li}^+$  (mol. w./charge 6.941) and  $\text{Al}^{3+}$  (mol. w./charge 8.99) in column experiments. The adsorption curves of Li and Al have long tails, which makes estimation of the capacity difficult.

The adsorption of  $\text{Na}^+$  and  $\text{Cr}^{3+}$  was approximately the same in the two experiments. The shaking experiment seemed to be slightly more efficient for  $\text{Fe}^{3+}$ , which may be due to hydroxide formation. At pH 3.3,  $\text{Fe}(\text{OH})_3$  colloids may exist. The column experiment was more efficient for the other cations.

#### 3.4.2.3 Interpretation of the results

The values of the capacities and calculated parameters are collected in Table XII. The results from the experiments with  $\text{NH}_4^+$ ,  $\text{NO}_3^-$  and  $\text{H}_2\text{PO}_4^-$  are deficient because the capacities were either very small ( $\text{H}_2\text{PO}_4^-$ ) or below detection limit ( $\text{NH}_4^+$  and  $\text{NO}_3^-$ ) at pH 3.3. The descending parts of the curves obey well the first order kinetic

Table XII. The parameters calculated from adsorption curves for Rastuonsuo peat.

Cation	Flow rate $\mu\text{eq}/100 \text{ g x s}$	Capacity o meq/100 g x		$\log K_{\text{comp}}$	$\log K_{\text{kin}}$	Regression	$t^{-1}$
Mn <sup>2+</sup>	1.7	13.7	8.3	-0.22	-3.76	0.999	4010
Ni <sup>2+</sup>	1.6	15.7	6.2	-0.25	-3.80	1.0	4360
Co <sup>2+</sup>	1.6	13.6	6.2	-0.34	-3.70	1.0	3440
Zn <sup>2+</sup>	1.4	14.4	8.2	-0.38	-3.76	0.992	3980
Cd <sup>2+</sup>	1.7	14.3	9.0	-0.37	-3.68	1.0	3320
Cu <sup>2+</sup>	3.0	20.2	16.0	-0.19	-3.51	1.0	2270
Pb <sup>2+</sup>	1.8	27.0	20.0	-0.24	-3.87	1.0	5130
Li <sup>+</sup>	6.8	7.0	1.7	-	-2.94	0.993	610
Na <sup>+</sup>	2.0	2.3	2.7	-	-3.27	0.997	1280
K <sup>+</sup>	1.2	2.3	1.8	-	-3.00	0.998	700
Mg <sup>2+</sup>	3.9	9.7	5.6	0.46	-3.43	0.991	1840
Ca <sup>2+</sup>	2.3	6.7	4.9	-	-3.42	1.0	1820
Sr <sup>2+</sup>	5.4	20.7	15.8	0.08	-3.41	0.998	1770
Ba <sup>2+</sup>	0.7	2.6	2.0	-1.2	-3.21	0.994	1140
Ag <sup>+</sup>	0.9	7.8	6.8	-0.02	-4.08	0.999	8340
Hg <sup>2+</sup>	2.8	16.2	5.1	0.63	-3.73	0.995	3680
Al <sup>3+</sup>	10	30.8	3.3	0.38	-3.18	1.0	1060
Cr <sup>3+</sup>	5.8	26.6	26.5	0.17	-3.50	0.999	2190
Fe <sup>3+</sup>	15	35.2	38.4	0.50	-3.24	0.988	1190

o = column experiment  
x = shaking experiment

equation.  $\text{Fe}^{3+}$  is an exception, perhaps due to hydroxide formation. The order of the adsorption is in column experiments  $\text{Fe}^{3+} > \text{Al}^{3+} > (\text{Pb}^{2+}) \sim \text{Cr}^{3+} > \text{Sr}^{2+} \sim (\text{Cu}^{2+}) > \text{Hg}^{2+} \sim \text{Ni}^{2+} > \text{Zn}^{2+} \sim \text{Cd}^{2+} \sim \text{Mn}^{2+} \sim \text{Co}^{2+} > \text{Mg}^{2+} > \text{Ag}^+ > \text{Li}^+ \sim \text{Ca}^{2+} > \text{Ba}^{2+} \sim \text{Na}^+ \sim \text{K}^+$ . The corresponding order in shaking experiments is  $\text{Fe}^{3+} > \text{Cr}^{3+} > (\text{Pb}^{2+} > \text{Cu}^{2+}) \sim \text{Sr}^{2+} > \text{Cd}^{2+} \sim \text{Mn}^{2+} \sim \text{Ni}^{2+} \sim \text{Zn}^{2+} > \text{Ag}^+ > \text{Co}^{2+} > \text{Mg}^{2+} > \text{Hg}^{2+} \sim \text{Ca}^{2+} > \text{Al}^{3+} > \text{Na}^+ > \text{Ba}^{2+} > \text{Li}^+ \sim \text{K}^+$ .

The values of  $K_{\text{comp}}$  provide a rough estimate of the capacities, with a few exceptions. The values of  $K_{\text{kin}}$  and  $t_{\frac{1}{2}}$  depend on the flow rate and so the values of these parameters can be compared only for  $\text{Mn}^{2+}$ ,  $\text{Ni}^{2+}$ ,  $\text{Co}^{2+}$ ,  $\text{Zn}^{2+}$ ,  $\text{Cd}^{2+}$  and  $\text{Pb}^{2+}$ , whose flow rates were comparable.

The exchange capacity of peat for trivalent ions has received only minor attention in the literature because the experiments must be performed at rather low pH to prevent hydroxide formation. Puustjärvi /50/ predicted a strong capacity of peat for trivalent ions based upon the theory of Donnan /51/.

There is some information in the literature concerning the adsorption of uni- and divalent ions on peat, but the experiments have mostly been carried out by static method (with no flow through the sample) using concentrated solutions, with the purpose of obtaining maximum filling of the vacant sites in peat.

Bunzl et al. /52/ compared the adsorption of several heavy metal ions and  $\text{Ca}^{2+}$  on Sphagnum peat. The method used was a static stirring experiment, where the ion exchange rate for a hydrogen saturated sample was followed by continuous pH measurement after mixing the cation solution with peat. The amounts bound were confirmed by atomic adsorption spectrophotometry. The results were compared using curves where the distribution coefficient calculated by Eq. 30 was plotted as a function of the total cation concentration in the solution.

$$K_{d, Me} \text{ (cm}^3/\text{g)} = \frac{\bar{n} \text{ Me}}{n \text{ Me}} \quad (30)$$

where

$\bar{n} \text{ Me}$  = the molal concentration of  $\text{Me}^{2+}$  ions in dry peat

$n \text{ Me}$  = the molal concentration of  $\text{Me}^{2+}$  ions in solution

$K_d$  = distribution coefficient

The order of the selective uptake was the same independent of the concentration:  $\text{Pb}^{2+} > \text{Cu}^{2+} > \text{Cd}^{2+} \sim \text{Zn}^{2+} > \text{Ca}^{2+}$  at pH 3.5 - 4.5. The order is the same as that obtained in this work in different conditions.

According to Belkevich and co-workers /17/ who used a static method and concentrated solutions (0.1 mole/dm<sup>3</sup>, pH ~ 6) the order of adsorption of divalent ions on peat is  $\text{Cu}^{2+} > \text{Co}^{2+} > \text{Zn}^{2+} > \text{Ni}^{2+} > \text{Ba}^{2+} > \text{Sr}^{2+} > \text{Ca}^{2+} > \text{Mg}^{2+}$ . The corresponding order of univalent ions is  $\text{Ag}^+ > \text{Tl}^+ > \text{Cs}^+ > \text{K}^+ > \text{Na}^+ > \text{Li}^+$ . The capacity order of alkaline earths obtained in our work differs from that of Belkevich et al. but the order of univalent cations is the same. Their use of Cu and Ni solutions of pH 6 is questionable because at that pH there probably exist hydroxide colloids.

Rathsack et al. /53/ and Jungk /54/ studied adsorption of uni- and divalent ions on H<sup>+</sup>-saturated peat. The pH was 5 in the former study and varied in the latter work. The concentration was 0.01 mole/dm<sup>3</sup>.

According to Rathsack et al. the order of adsorption on peat is with low saturation level  $\text{Ba}^{2+} > \text{Ca}^{2+} > \text{Mg}^{2+} \gg \text{K}^+ > \text{NH}_4^+ > \text{Na}^+$  and with high saturation level  $\text{Ca}^{2+} > \text{Ba}^{2+} > \text{Mg}^{2+} > \text{NH}_4^+ > \text{K}^+ \sim \text{Na}^+$ .

The order is different from that of Tummavuori et al. /49/. Especially their results for  $\text{NH}_4^+$  adsorption is surprising.



The adsorption order of divalent heavy metals seems to be the same independent of the method, concentration and pH of the solution. Likewise the order of the alkalies is nearly constant. The adsorption order of alkaline earths, on the other hand, is sensitive to conditions, except for  $\text{Sr}^{2+}$ , which was consistently adsorbed with high selectivity. The order of trivalent ions has not been reported before.

To compare the results with those of chelating resins the results of static experiments performed with Polyacrylamidoxime resin by Colella and his co-workers /55/ have been expressed. The order and capacities (meq/100 g resin) at pH 5 are as follows:  $\text{Cu}^{2+}$  (290) >  $\text{Hg}^{2+}$  (214) >  $\text{Ag}^{2+}$  (156) >  $\text{Pb}^{2+}$  (144) >  $\text{Ni}^{2+}$  (80) >  $\text{Zn}^{2+}$  (76) >  $\text{Co}^{2+}$  (68) >  $\text{Cd}^{2+}$  (38) >  $\text{Mn}^{2+}$  (26). In addition, the experiments with iron were carried out at pH 2 and the corresponding results are:  $\text{Fe}^{3+}$  (255) >  $\text{Fe}^{2+}$  (48). The complexing of  $\text{Cu}^{2+}$  and  $\text{Ag}^+$  is strikingly strong. The coefficient of difference between the values in Table XII is with  $\text{Cu}^{2+}$  14 and  $\text{Mn}^{2+}$  2. The order  $\text{Cu}^{2+}$  >  $\text{Ni}^{2+}$  >  $\text{Zn}^{2+}$  ~  $\text{Co}^{2+}$  is the same than that of column experiments in Table XII. Colella followed also capacity changes with increasing pH and the tendency was usually increasing. The capacity of  $\text{Hg}^{2+}$  was not clearly pH-dependent between pH 2 - 6. Measurements with  $\text{Cu}^{2+}$  and  $\text{Ni}^{2+}$  were performed up to pH value 9, that is questionable because of hydroxide formation. For example the capacity of  $\text{Cu}^{2+}$  was found to decrease with increasing pH after pH value 5.5

#### 3.4.3 Adsorption of $\text{Cu}^{2+}$ , $\text{Sr}^{2+}$ , $\text{Ca}^{2+}$ and $\text{K}^+$ on pure Sphagnum peat species

The peat in wetlands is a combination of several peat species and the composition is not always easy to analyze. To get more thorough knowledge of the adsorption capacity of Sphagnum-type peat at pH 3.3, five pure Sphagnum peats were chosen for study /39/.

The studied subsamples represented the following peats: S. Cuspidata (H1-2), S. Cuspidata (H3), S. Fuscum (H2), S. Fuscum (H3) and S. Palustris (H1-2).

The concentrations of the test solutions are shown in Table XIII.

Table XIII. The concentrations of the solutions used in adsorption experiments.

Cation	Mol. wt./ charge	mg/cm <sup>3</sup>	Concentration meq/dm <sup>3</sup>	pH
Cu <sup>2+</sup>	31.77	100	3.15	3.3
Sr <sup>2+</sup>	43.81	250	5.71	3.3
Ca <sup>2+</sup>	20.04	50	2.50	3.3
K <sup>+</sup>	39.09	50	1.28	3.3

#### 3.4.3.1 Adsorption curves

The adsorption curves of the cations at pH 3.3 are shown in Figures 30, 31, 32 and 33.

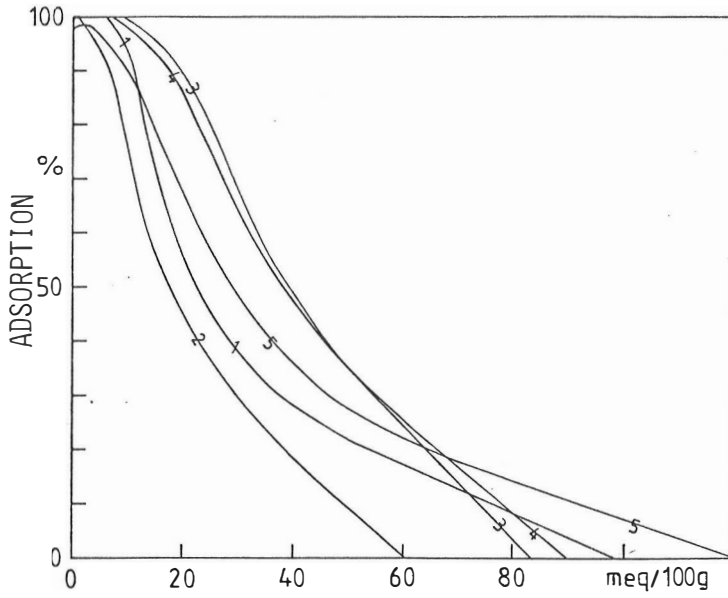


Figure 30. Adsorption curves of  $\text{Cu}^{2+}$ . Codes:  
1 = S. Cuspidata H1-2, 2 = S. Cuspidata H3,  
3 = S. Fuscum H2, 4 = S. Fuscum H3,  
5 = S. Palustria H1-2

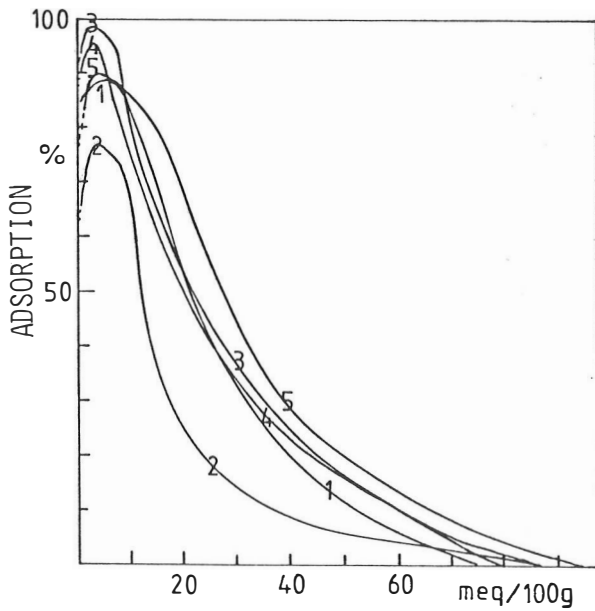


Figure 31. Adsorption curves of  $\text{Sr}^{2+}$ .

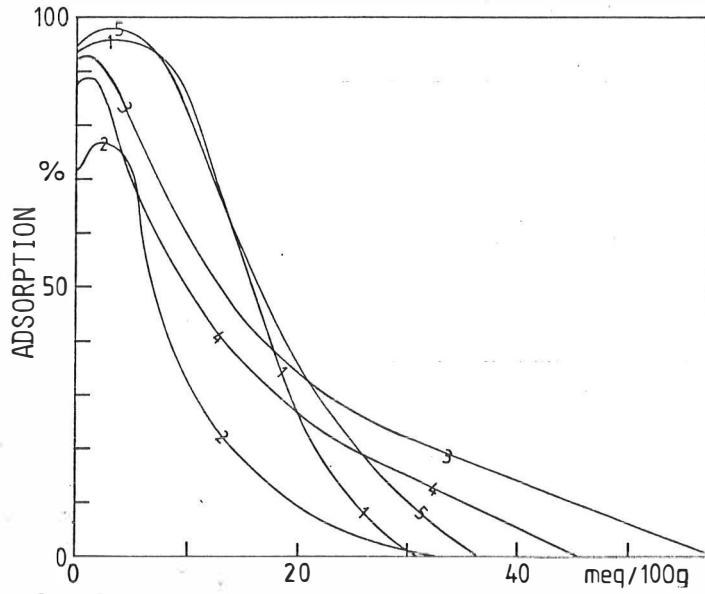


Figure 32. Adsorption curves of  $\text{Ca}^{2+}$ .

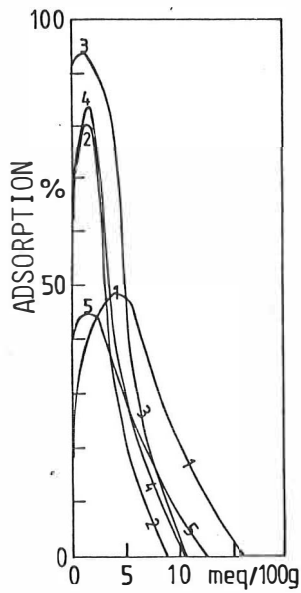


Figure 33. Adsorption curves of  $\text{K}^{+}$ .

### 3.4.3.2 Comparison of the adsorptions

The parameters calculated from the adsorption curves are listed in Table XIV. The order of adsorption was the same for all the peat types studied:  $\text{Cu}^{2+} > \text{Sr}^{2+} > \text{Ca}^{2+} > \text{K}^+$ . The order of capability to adsorb the cations is for  $\text{Cu}^{2+}$ : S. Fuscum H2 ~ S. Fuscum H3 > S. Palustria H1-2 > S. Cuspidata H1-2 > S. Cuspidata H3; for  $\text{Sr}^{2+}$ : S. Palustria H1-2 > S. Fuscum H2 > S. Fuscum H3 ~ S. Cuspidata H1-2 > S. Cuspidata H3; for  $\text{Ca}^{2+}$ : S. Fuscum H2 ~ S. Palustria H1-2 ~ S. Cuspidata H1-2 > S. Fuscum H3 > S. Cuspidata H3; for  $\text{K}^+$ : S. Fuscum H2 > S. Cuspidata H1-2 > S. Fuscum H3 > S. Cuspidata H3 ~ S. Palustria H1-2.

S. Cuspidata H3 has the weakest ion exchange capability. If the adsorption ability of the cation is strong (for example,  $\text{Cu}^{2+}$ ) the capacities of S. Fuscum H2 and H3 are almost equal, despite the high mineral concentration in the latter sample. If the cation has weak binding ability (as  $\text{K}^+$ ) the original cation concentration probably has an effect, and the capacity values of the S. Fuscum peats differ. The original potassium content of S. Cuspidata H1-2 is high and during the first few minutes of the flow of  $\text{K}^+$  solution through the sample, part of the natural potassium was released. After this step the peat adsorbed potassium with relatively low adsorption level (figure 32 curve 1). Practically no potassium was released by pure 0.0005 mol/dm<sup>3</sup>  $\text{HNO}_3$  solution.

The descending parts of the curves usually obey well the first order kinetic equation. With S. Cuspidata H3 the regression coefficient is not very good (0.990).

The values of  $\log K_{\text{comp}}$  and  $\log K_{\text{kin}}$  usually reveal the adsorption order. The values of  $\text{Ca}^{2+}$  with S. Fuscum species are an exception to the rule, because of the long tailing of the adsorption curves. The values of  $K_{\text{comp}}$  do not always become stabilized with  $\text{K}^+$  because of the small capacity.

Table XIV. The values of parameters calculated from column experiments

Sample	Cation	Flow rate $\mu\text{eq}/100\text{gxs}$	Capacity $\text{meq}/100\text{ g}$	$\log K_{\text{comp}}$	$\log K_{\text{kin}}$	Regression	$t \frac{1}{2}$ s
1	$\text{Cu}^{2+}$	6.8	32.8	0.67	-3.58	0.999	3210
2	"	4.5	22.7	0.44	-3.70	1.000	3470
3	"	4.1	43.1	0.32	-3.87	1.000	5170
4	"	4.2	43.1	0.42	-3.90	1.000	5440
5	"	7.9	38.7	0.73	-3.60	1.000	2760
1	$\text{Sr}^{2+}$	11.6	25.1	0.48	-3.25	1.000	1240
2	"	9.2	16.1	0.57	-3.12	0.990	910
3	"	7.3	27.5	0.50	-3.55	1.000	2430
4	"	7.2	25.7	0.58	-3.55	1.000	2430
5	"	14.1	31.9	0.49	-3.21	0.999	1110
1	$\text{Ca}^{2+}$	5.0	15.9	-0.29	-3.18	0.997	1050
2	"	4.0	8.5	0.18	-3.28	0.996	1310
3	"	3.1	18.1	0.54	-3.77	0.999	4080
4	"	3.2	14.1	0.45	-3.69	1.000	3390
5	"	5.6	17.6	-0.09	-3.30	0.999	1380
1	$\text{K}^{+}$	2.6	4.4	-	-3.24	0.996	1200
2	"	2.1	3.1	-	-3.07	1.000	810
3	"	1.6	5.2	-0.67	-3.18	0.999	1050
4	"	1.6	3.8	-0.33	-3.30	0.999	1370
5	"	3.2	2.9	-	-3.11	0.996	900

### 3.4.3.3 Comparison with literature data

Some ion exchange capacity values have been published for Sphagnum type peats. The results are from static experiments with concentrated cation solutions and with samples presaturated with hydronium ion. According to Bunzl et al. /52/, the capacity values for several cations are as follows (meq/100 g):  $\text{Ca}^{2+}$  80,  $\text{Zn}^{2+}$  100,  $\text{Cd}^{2+}$  120,  $\text{Cu}^{2+}$  130 and  $\text{Pb}^{2+}$  130. The experiments were carried out at pH 4. In the collaborative study arranged by Thorpe /56/ the capacity values obtained for  $\text{Ba}^{2+}$  by the method by Puustjärvi /23/ varied between 118 and 127 meq/100 g. As can be seen the capacities do not differ markedly under forced conditions.

### 3.4.4 Relevance of sampling place

In this series of experiments the adsorption properties of low-moor peat samples from three production areas were compared. The effect of the degree of humification was studied with two samples from the same production area. It is certain that the samples are not totally representative of the production areas, because peat type can vary widely within the same bog.

The experiments were performed by column method, and the cations studied were  $\text{Pb}^{2+}$ ,  $\text{Cu}^{2+}$ ,  $\text{Zn}^{2+}$ ,  $\text{Sr}^{2+}$ ,  $\text{Ca}^{2+}$  and  $\text{Mg}^{2+}$  which represent heavy metals and alkaline earths. The concentrations of the solutions used are given in Table XV.

Table XV. The concentrations of the cation solutions.

Cation	mol. w./ charge	Concentration		pH
		mg/dm <sup>3</sup>	meq/dm <sup>3</sup>	
$\text{Pb}^{2+}$	103.60	200	1.93	2.9
$\text{Cu}^{2+}$	31.77	100	3.15	3.3
$\text{Zn}^{2+}$	32.69	50	1.53	3.3
$\text{Sr}^{2+}$	43.8	250	5.71	3.3
$\text{Ca}^{2+}$	20.04	50	2.50	3.3
$\text{Mg}^{2+}$	12.16	50	4.11	3.3

#### 3.4.4.1 Adsorption behaviour

The curves for the adsorption of  $Mg^{2+}$  and  $Sr^{2+}$  on low-moor samples are shown in Figure 34. The curves for  $Zn^{2+}$  and  $Pb^{2+}$  are in Figure 35 and those for  $Cu^{2+}$  and  $Ca^{2+}$  in Figure 36. Curves for peat from Rastunsuo (H5-6) are included in the figures for purposes of comparison. The parameters calculated from the adsorption curves of the low-moor peat samples are collected in Table XVI.

The reference peat (Rastunsuo H5-6) is seen to have the weakest capacity, except for  $Sr^{2+}$ .  $Cu^{2+}$  has the highest selectivity on the low-moor peats studied. In the case of  $Ca^{2+}$  the shapes of the adsorption curves differ significantly. The curves for  $Zn^{2+}$ ,  $Pb^{2+}$ , and  $Sr^{2+}$  are not greatly different in shape. The adsorption order on the low-moor samples is for sample 1 (see Table XVI)  $Pb^{2+} \sim Cu^{2+} \sim Sr^{2+} > Zn^{2+} > Ca^{2+} > Mg^{2+}$  and for sample 2  $Pb^{2+} \gg Cu^{2+} > Sr^{2+} \sim Zn^{2+} > Ca^{2+}$ . The tendency  $Pb > Cu$  is strong with sample 2, moderate with sample 3 and weak with sample 1. The capacity values for  $Cu^{2+}$  and  $Pb^{2+}$  (Table XVI) are seen to be nearly equal.  $Pb$  is more strongly adsorbed, however, because the pH value is lower in the  $Pb^{2+}$  solution than in the other solutions. The order of  $Ca^{2+}$  and  $Mg^{2+}$  varies with the sample. The two cations have almost equal binding abilities on samples 1 and 2 and  $Mg^{2+}$  is adsorbed strongly on sample 3.  $Sr^{2+}$  has strong binding ability sometimes even greater than the value of  $Zn^{2+}$  /56/.

The value of  $K_{comp}$  is small with  $Pb^{2+}$  because the descending parts of the curves are steep in relation to the high capacity. The curves of  $Pb^{2+}$  have a wide region of  $> 99.5$  % adsorption. The values of  $K_{kin}$  and  $K_{comp}$  are high with  $Mg^{2+}$  because the curves have long tails.



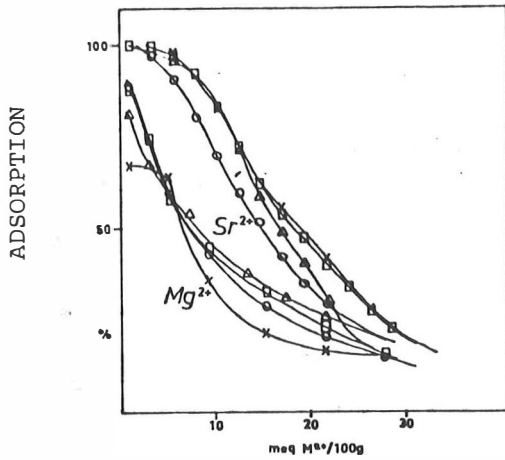


Figure 34. Adsorption curves of  $Sr^{2+}$  and  $Mg^{2+}$  on low-moor peat. Codes: x = peat H5-6 from Rastunsuo, o = peat H1-2 from Haukineva, □ = peat H1-2 from Aitoneva, Δ = peat H1-2 from Konnunsuo.

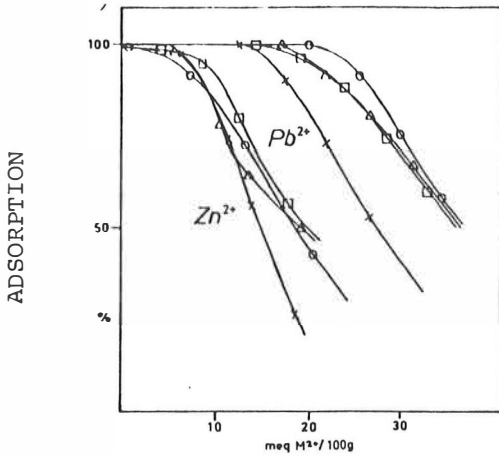


Figure 35. Adsorption curves of  $Zn^{2+}$  and  $Pb^{2+}$ . Codes as in Figure 34.

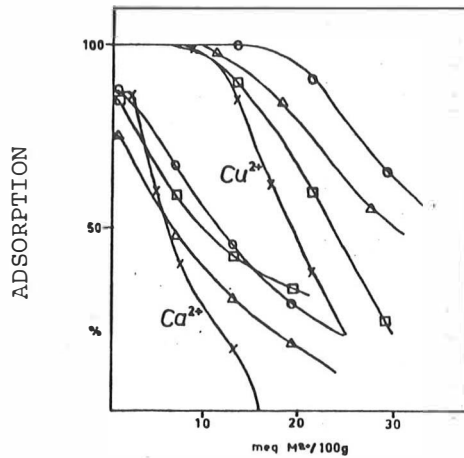


Figure 36. The adsorption curves of  $Cu^{2+}$  and  $Ca^{2+}$ . Codes as in Figure 34.

Table. XVI. The parameters calculated from adsorption curves for low-moor samples.

Sample	Cation	Flow rate $\mu\text{eq}/100\text{gxs}$	Capacity $\text{meq}/100\text{ g}$	$\log K_{\text{comp}}$	$\log K_{\text{kin}}$	Regression	$t_{\frac{1}{2}}$ s
1	Mg <sup>2+</sup>	6.0	13.5	0.55	-3.34	0.998	1510
2	"	4.8	14.4	0.53	-3.54	0.995	2410
3	"	4.8	13.8	0.67	-3.59	0.998	2670
1	Ca <sup>2+</sup>	3.7	14.3	0.37	-3.62	1.000	2870
2	"	2.9	13.9	0.65	-3.88	0.996	5230
3	"	2.8	9.0	0.46	-3.70	1.000	3490
1	Sr <sup>2+</sup>	8.4	19.9	0.33	-3.21	1.000	1120
2	"	6.7	20.9	0.11	-3.32	0.997	1450
3	"	6.7	18.6	-0.06	-3.16	1.000	1000
1	Cu <sup>2+</sup>	4.6	37.8	-0.11	-3.57	1.000	2570
2	"	3.7	23.0	-0.38	-3.44	0.999	1930
3	"	3.6	31.5	0.01	-3.74	0.999	3840
1	Pb <sup>2+</sup>	2.8	36.7	-0.25	-3.75	1.000	3940
2	"	2.3	35.3	-0.16	-3.87	1.000	5140
3	"	2.2	35.7	-0.17	-3.88	1.000	5220
1	Zn <sup>2+</sup>	2.3	18.8	-0.08	-3.73	0.999	3700
2	"	1.8	19.6	-0.19	-3.83	0.999	4650
3	"	1.7	20.0	0.13	-4.10	1.000	8600

Samples:

- 1: Haukineva H1-2
- 2: Aitoneva H1-2
- 3: Konnunsuo H1-2

Increase in the degree of humification affected slightly the ion exchange capacities of the samples (H1-2 and H4-5 from the same production area). The change was for Ca +13 %, for Zn +11 % and for Cu +10 %.

#### 3.4.5 The effect of two pretreatment methods on adsorption properties of peat

##### 3.4.5.1 Effect of freezing

The effect of freezing was studied with medium-moor peat (H4-6) from the Konnunsuo production area. The samples were frozen at 255 K with two different water contents: 80 % and 95 % by weight. After freezing, the samples were kept in a freezer for several days /57/.

The cations studied were  $\text{Cu}^{2+}$ ,  $\text{Zn}^{2+}$ ,  $\text{Ca}^{2+}$  and  $\text{K}^+$ , and concentrations of the solutions were  $\text{Cu}^{2+}$  3.15 meq/dm<sup>3</sup> (100 mg/dm<sup>3</sup>),  $\text{Zn}^{2+}$  1.53 meq/dm<sup>3</sup> (50 mg/dm<sup>3</sup>),  $\text{Ca}^{2+}$  2.50 meq/dm<sup>3</sup> (50 mg/dm<sup>3</sup>) and  $\text{K}^+$  1.28 meq/dm<sup>3</sup> (50 mg/dm<sup>3</sup>). Experiments were carried out by column method at pH 3.3.

The effect of freezing depended on the ion and on the water content of the peat. The water content 80 % was usually too small to break the structure of peat. Only with zinc there was a small increase in capacity. Water content of 95 % was sufficient to break the structure during freezing and thus probably increased the surface area of peat. The phenomenon can be observed in Figures 37 and 38 as broadening of the region with adsorption > 99.5 %. The effect was evident for  $\text{Zn}^{2+}$  and  $\text{Cu}^{2+}$ .

The freezing and the changes in structure had no effect on the adsorption of  $\text{K}^+$ . The effect on the adsorption of  $\text{Ca}^{2+}$  was different than the effect on  $\text{Cu}^{2+}$  and  $\text{Zn}^{2+}$ . The curves for  $\text{Ca}^{2+}$  differed in regions of low adsorption per cent, with freezing slightly increasing the adsorption. With untreated sample part of the bound  $\text{Ca}^{2+}$  was released after saturation; this was not found with frozen samples.

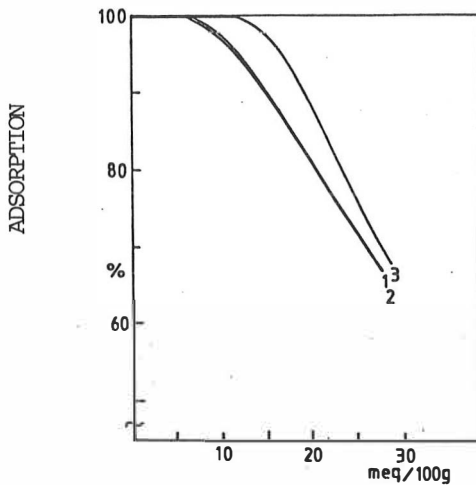


Figure 37.  
The effect of freezing on the adsorption curves of  $\text{Cu}^{2+}$ .  
1 = unfrozen, 2 = frozen with 80 %  $\text{H}_2\text{O}$ , 3 = frozen with 95 %  $\text{H}_2\text{O}$ .

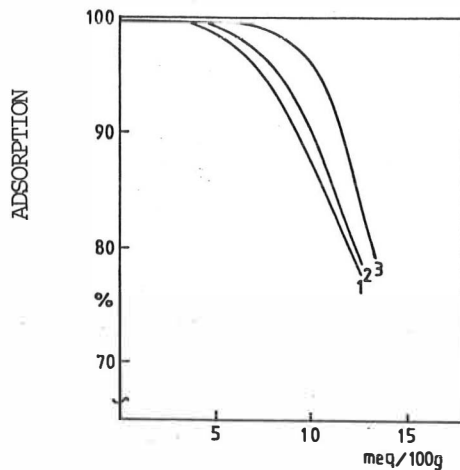


Figure 38.  
The effect of freezing on the adsorption curves of  $\text{Zn}^{2+}$ . Codes as in Figure 37.

#### 3.4.5.2 Effect of extracting part of the long chain hydrocarbons

The extraction experiments were carried out with benzene - ethanol mixture (80:20), which is an effective extractant for long-chain hydrocarbon compounds (waxes, resins). The two samples studied were the same as in section 3.2.1. The extraction was performed after drying at room temperature (293 K) to final moisture content 6 - 7 %, or after drying in a furnace at 376 K. The method of drying had no influence on the adsorption curves.

The adsorption curves of untreated and extracted samples are compared in Figure 39. The cation solution used was  $\text{Cu}^{2+}$  3.15 meq/dm<sup>3</sup> (100 mg/dm<sup>3</sup>) pH = 3.0.

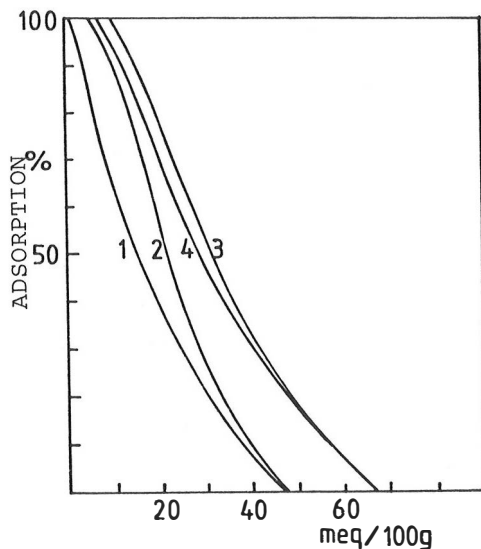


Figure 39. Adsorption curves of samples with  $\text{Cu}^{2+}$ -solution. 1 = untreated sample from Rastunsuo, 2 = same sample after extraction, 3 = untreated sample from Haukineva, 4 = same sample after extraction.

The change in the adsorption depended on the sample. Extraction increased the capacity of the medium-moor sample, which contained more bitumens. The capacity of the low-moor sample with low concentration of bitumens decreased slightly, indicating the undesirable effect of extraction on the adsorption sites.

Stronger extractants such as NaOH would probably have stronger effects on the capacity. Such reagents were not used in this study because of their destructive effect on the physical structure of peat.

#### 3.4.6 Multi-cation experiments

The multi-cation experiments were divided into two parts: a) column experiments where  $\text{Zn}^{2+}$  was forced out of peat with  $\text{Cu}^{2+}$ , b) shaking experiments with solutions containing several cations.

### 3.4.6.1 Forcing-out experiment

The  $\text{Cu}^{2+}$ - $\text{Zn}^{2+}$  forcing-out experiment was performed to study the release of one cation of moderate adsorption ability by cation of higher ability. The peat samples were the same as in section 3.1.1.

The concentrations of the cation solutions used in these three-step experiments were  $\text{Cu}$   $100 \text{ mg/dm}^3$  ( $3.15 \text{ meq/dm}^3$ ),  $\text{pH}$  3.0 and  $\text{Zn}$   $105 \text{ mg/dm}^3$  ( $3.21 \text{ meq/dm}^3$ ),  $\text{pH}$  3.0. The first step was saturation of the peat column with a large volume of the  $\text{Zn}^{2+}$  solution. The second step was washing out of the unbound zinc with  $0.001 \text{ mol/dm}^3 \text{ HNO}_3$  solution ( $\text{pH} = 3.0$ ). And the third step was allowing the copper solution to flow through the columns.  $\text{Zn}^{2+}$  and  $\text{Cu}^{2+}$  were then determined in the column effluents. The adsorption curves of  $\text{Cu}^{2+}$  compared with those of untreated samples are shown in Figure 40.

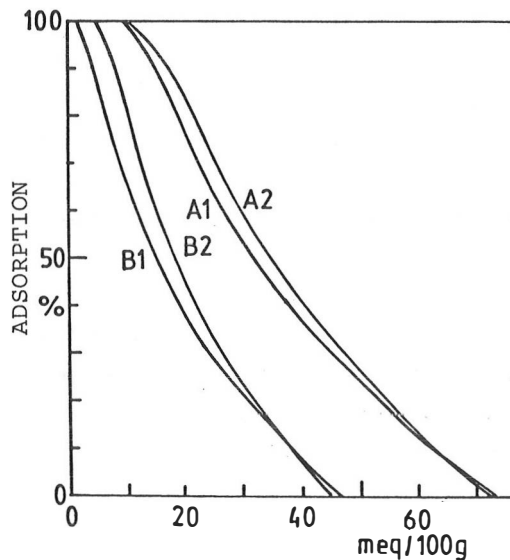


Figure 40. The adsorption curves of  $\text{Cu}^{2+}$  from the forcing-out experiments. A = sample H1-2 from Haukineva, B = sample H5-6 from Rastunsuo, 1 = untreated, 2 = after saturation with  $\text{Zn}^{2+}$ .

The parameters calculated from the adsorption curves are collected in Table XVII.

Table XVII. Parameters calculated from the adsorption curves of the forcing-out experiments.

Sample	Capacity meq/100 g	$\log K_{\text{comp}}$	$\log K_{\text{kin}}$	Regression	$T\frac{1}{2}$ s
A1	35.9	0.32	-3.76	1.000	5310
A2	37.5	0.21	-3.73	1.000	5350
B1	17.7	0.39	-3.89	1.000	3730
B2	20.0	0.12	-3.86	1.000	3960

A = peat H1-2 from Haukineva      1 = untreated  
 B = peat H5-6 from Rastunsuo      2 = saturated with  $\text{Zn}^{2+}$

The  $\text{Cu}^{2+}$  capacity increased slightly after  $\text{Zn}^{2+}$  saturation. The values of  $K_{\text{comp}}$  and the absolute values of  $K_{\text{kin}}$  decreased slightly, indicating steeper slopes in the curves.

Figure 41 shows the release of  $\text{Zn}^{2+}$  and adsorption of  $\text{Cu}^{2+}$  as a function of the amount of copper passed through the column. The curves from two identical experiments with sample A allow an estimate of the reproducibility.

Figure 41 reveals that  $\text{Cu}^{2+}$  forces  $\text{Zn}^{2+}$  out nearly quantitatively.

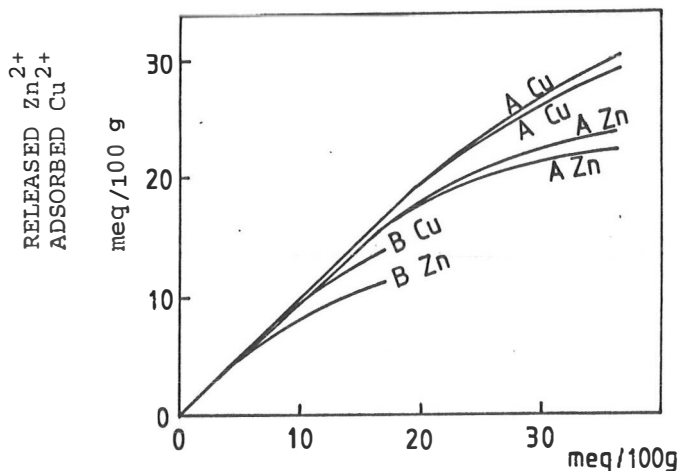


Figure 41. The amounts of released  $Zn^{2+}$  and adsorbed  $Cu^{2+}$ .

#### 3.4.6.2 Shaking experiments

Shaking experiments with solutions containing several cations were carried out with two peat samples: peat H5-6 from Rastunsuo and peat H7-8 from Jouttenuisenneva. The solutions contained seven divalent heavy metals and the concentrations were adjusted to represent the composition of possible waste water, pH 3.0: Cd 0.50 mg/dm<sup>3</sup>, Cu 2.50 mg/dm<sup>3</sup>, Ni 2.50 mg/dm<sup>3</sup>, Co 2.50 mg/dm<sup>3</sup>, Pb 4.00 mg/dm<sup>3</sup>, Zn 1.00 mg/dm<sup>3</sup> and Mn 1.00 mg/dm<sup>3</sup>. The amount of peat calculated on a dry weight basis varied between 1 and 9 % in the mixtures. The volume of the added cation solution was 100 cm<sup>3</sup> and the shaking time was 22 hours. The total water content in the mixture was about 100 cm<sup>3</sup> plus the water bound in the peat. The results from the experiments are shown in Figures 42 and 43, where the adsorbed part of the cation (as per cents) is presented as the ordinate and the peat content as the abscissa.



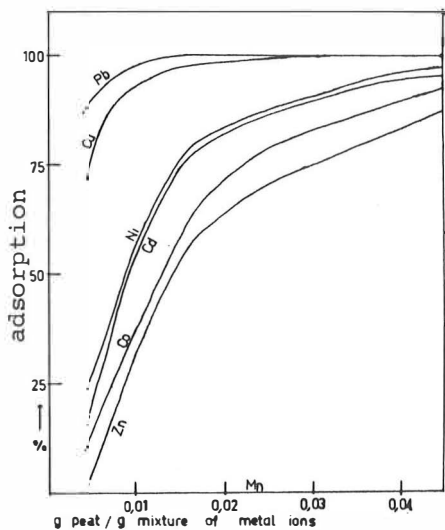


Figure 42.

The results from shaking experiments with the sample from Jouttensisenneva.

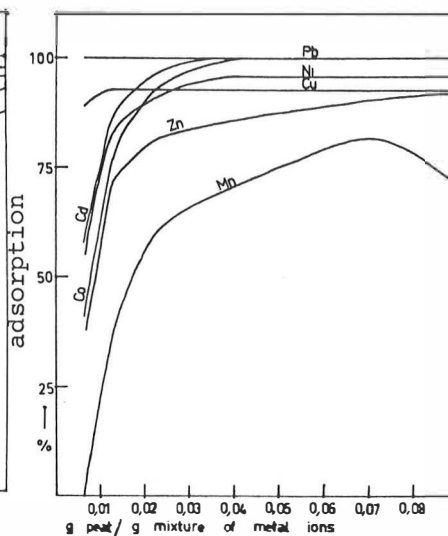


Figure 43.

The results from shaking experiments with the sample from Rastunsuo.

Lead was the strongest cation in competition for the adsorption sites.  $Mn^{2+}$  had the weakest ability to adsorb on the samples. Owing to the high  $Mn^{2+}$  content of the sample from Jouttensisenneva no  $Mn^{2+}$  adsorption is seen in Figure 42. The sample from Rastunsuo was the stronger adsorber of divalent heavy metals.

### 3.4.7 Peat as a cation filter

Peat adsorbs cations much like ion exchange resins and can thus be utilized for selective removal of cations from solution. Typical pollutants like divalent heavy metals have relatively high affinities on peat which favours its use as a wastewater filter. Common cations like  $K^+$ ,  $Na^+$  and  $Ca^+$  have rather low affinities, which favours the same purpose.  $Fe^{3+}$  is a common ion with a strong binding ability, which could have an undesirable effect in filter use.

The case of  $\text{Sr}^{2+}$  (an important component in nuclear wastes) is interesting: it was found to have a great selectivity in the non-forced adsorption conditions used in this study.

#### 3.4.7.1 Repeated use of a larger peat layer

To study the use of peat as cation filter in larger scale, experiments were carried out with a layer 580  $\text{cm}^3$  in volume, 19 cm in height and 6.25 cm in diameter. The volume was 36 times greater than used in other experiments. The peat used in the experiments was sample H1-2 from Haukineva, because this sample was found to have a high capacity for toxic cations at adsorption level  $> 99.5\%$ . This sample also allowed use of a rather high flow rate of solution through the column because of the low degree of humification and consequent large mean particle size.

The parameters studied were the influence of the first and repeated elutions and washings on the adsorption curves, capacities and maximum flow rate through the column. The volumes of eluent (1 mole/ $\text{dm}^3$   $\text{HNO}_3$ ) and washing water needed were also measured. The flow rate of the  $\text{Cu}^{2+}$  solution  $C = 3.15 \text{ meq}/\text{dm}^3$  (100  $\text{mg}/\text{dm}^3$ ) pH 3.0 was kept at a constant value of 16  $\mu\text{eq}/100\text{gxs}$  which corresponds to the value 2.08  $\text{cm}^3/\text{s}$ . The volumes of effluent fractions for determinations were 1000  $\text{cm}^3$ . In more precise elution studies the volume of one fraction was 250  $\text{cm}^3$ . The total volume of the  $\text{Cu}^{2+}$  solution used during one experiment was 10  $\text{dm}^3$ .

The adsorption curves for the experiments are collected in Figure 44; the curve obtained with a small column is included for purposes of comparison.

The parameters calculated from the adsorption curves are listed in Table XVIII.

The adsorption curves and Table XVIII show that enlargement of the column had very little effect on the capacity; however the shapes of the curves show large columns to be

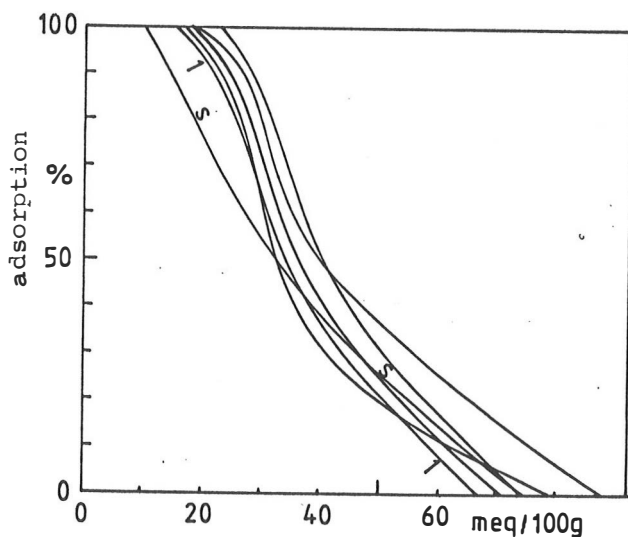


Figure 44. The adsorption curves with large column.  
1 untreated, S = with normal column, unmarked  
= after elutions.

more promising for water treatment purposes because the ability to adsorb copper at the level of  $> 99.5\%$  increased. The increased values of  $K_{comp}$  and decreased absolute values of  $K_{kin}$  and  $t_{\frac{1}{2}}$  (Table XVIII) indicate steeper descending regions in the adsorption curves of large columns (one exception). The tendency can also be seen in Figure 44.

The first elution increased the capacity only about 10%. After several elutions the values of the capacities were  $41.9 \pm 4.7$  meq/100 g. When the capacity was low (experiments 1,2 and 1,4 in Table XVIII) the descending regions of the curves obeyed poorly the first order kinetic equation. With untreated samples and in experiments with high capacity the regression coefficient was high.

The copper bound on the column was eluted sharply and the release was nearly complete after flow through of an eluent volume twice the volume of the peat column. Figure 45 shows the result compared with that obtained by Sugii /58/ and co-workers with macroreticular resin.

Table XVIII. The properties of large column.

Column	Capacity meq/100 g	Adsorption with > 99.5 % meq/100 g	$\log K_{\text{comp}}$	$\log K_{\text{kin}}$	Regression	$t_{\frac{1}{2}}$ 2
s,u *	35.7	9.7	0.36	-3.16	1.000	1000
1,u	37.3	14.4	0.01	-3.07	1.000	810
1,1	40.3	17.6	-0.02	-3.07	0.999	820
1,2	38.9	16.0	0.22	-3.15	0.985	970
1,3	46.5	19.0	0.26	-3.27	0.997	1270
1,4	37.1	16.2	0.14	-2.96	0.989	650
1,5	44.1	22.2	-0.05	-3.08	1.000	830

s = small column 16 cm<sup>3</sup>  
 l = large column 580 cm<sup>3</sup>  
 u = untreated

n (1, 2...5) = after n elutions with 1 mol/dm<sup>3</sup> HNO<sub>3</sub>  
 \* = flow rate = 20 µeq/100 gxs

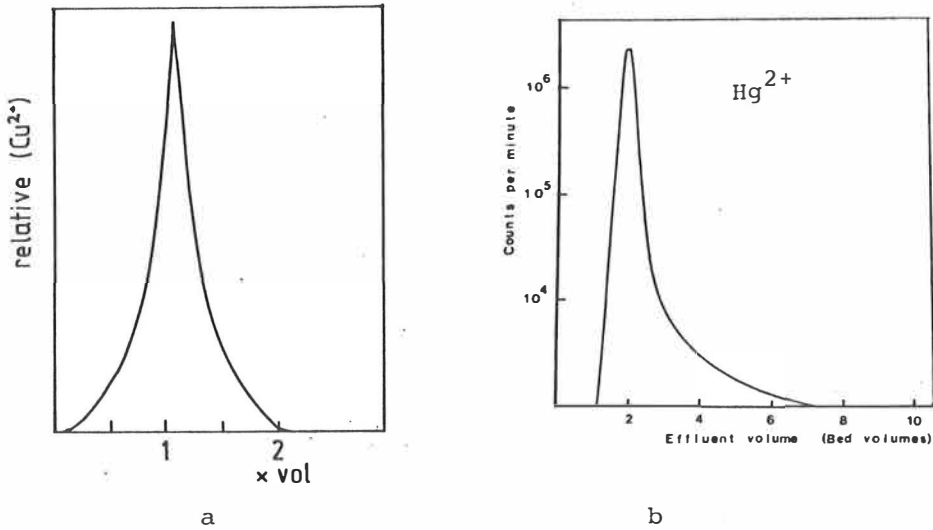


Figure 45. a) The releasing curve of  $\text{Cu}^{2+}$  during elution. Abscissa = the volume of the eluent (x volume of the peat column). b) The corresponding curve of  $\text{Hg}^{2+}$  /58/. Eluent = 0.1 M HCl.

The volume of washing water needed to increase the pH value to 4 after elution was about three times the volume of the column.

Repeated use influenced the physical state of the peat and decreased the maximum flow rate measured during washing. The tendency is shown by Figure 46. The level of maximum flow rate became stabilized after four elutions.

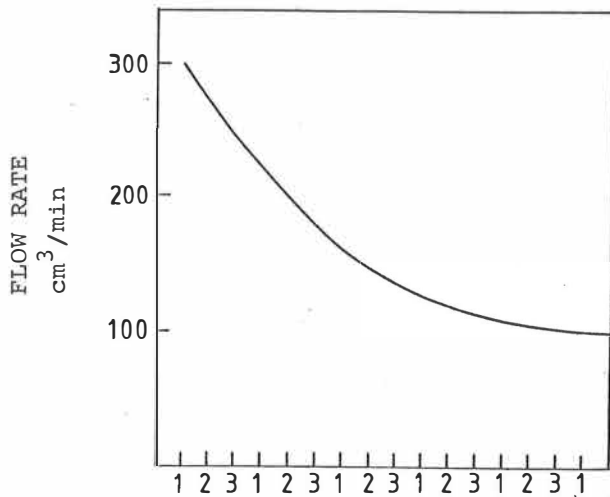


Figure 46. The influence of repeated use on the maximum flow rate. 1 = Cu adsorption, 2 = elution, 3 = washing.

## CONCLUSIONS

The adsorption of cations (alkalies excluded) from flowing test solution onto peat layer was at first almost complete in the conditions used (pH 3.0 - 3.3). After a certain point the adsorption capacity decreased according to the first order kinetic equation. The adsorption of anions was very weak in the pH range used.

The binding mechanism varied from nearly pure proton-cation exchange to almost complete cation-cation exchange. The adsorption capacity was strongly dependent on the cation type, pH of the test solution and sample type.

The order of adsorption capacity of divalent transition metals follows the complex stability order published earlier. The order of alkalies and alkaline earths is usually dependent on molecular weight such that adsorption decreases with increasing molecular weight. Strontium is a striking exception, which proves the selectivity of peat. Adsorption of trivalent cations on peat is strong.

The natural cation contents in pure Sphagnum peats vary widely. If alkalies are excluded, S. Fuscum is usually the strongest adsorber and S. Cuspidata the weakest.

Although pretreatment was usually avoided because it changes the structure of the sample from its original state, some freezing and extraction experiments were performed. Freezing elongates the region of high adsorption if the water content of the sample is sufficiently high.

Like an ion exchange resin, a peat layer can be used repeatedly as a cation filter, like ion exchange resins. Low-moor peat is most suitable because of its fibrous structure and consequent greater permeability to solutions. The adsorption capacity of low-moor samples tends to be high relative to other peat samples, though low relative to ion exchange resins.

The results provide information useful for estimating the effects and complex formation when sewage sludge containing pollutants and common cations is mixed with peat, when acid rain lowers the pH of peatland and when cations are concentrated in peat bogs through either rain water or flowing water. The value of a study of larger peat columns for heavy metal filtration is suggested, especially of the changes in maximum flow rate during repeated use of peat layers and the selection of the peat. Cost analyses are now needed to compare the advantages of peat with those of ion exchange resins.

REFERENCES

1. V. Puustjärvi, Kasvuturve ja sen käyttö, Turveteollisuusliitto r.y., Helsinki (1973).
2. R. Ruuhijärvi, Suomen suot ja niiden käyttö, Suoseura r.y., Helsinki 24 (1983).
3. K. Tolonen, Suomen suot ja niiden käyttö, Suoseura r.y., Helsinki 29 (1983).
4. L. von Post, " Inter. Soil Sci. Congr." Helsinki (1924).
5. J. Sarasto, Acta For. Fenn. 71, 16 (1960).
6. State standard of the USSR. International Peat Society, Helsinki, Finland 59 (1976).
7. R.S. Farnham, Management Assessment of Peat as an Energy Resource, Virginia, U.S.A 7 (1979).
8. E. Ekman, Kem-Kemi 9, 157 (1982).
9. W. Oswald, Kolloid-Z. 29, 316 (1921).
10. G.E. Boyd, A.W. Adamson and J. Myers, Jr., J. Am. Chem. Soc. 69, 2836 (1947 ), J.A. Marinsky, Ion Exchange I, Marcel Dekker inc., New York 67 (1966).
11. Z. Nernst, Physik. Chem. 47, 52 (1904), J.A. Marinsky, Ion Exchange I.
12. A. Vogelpohl, Symposium of Computers in the Design and Erection of Chemical Plants, Karlovy Vary 565 (1975).
13. T.R. Kressman and J.A. Kitchener, Discussions Faraday Soc. 7, 90 (1947 ), J.A. Marinsky, Ion Exchange I.
14. G. Eisenman, Membrane Transport and Metabolism, Academic Press, New York 163 (1961), J.A. Marinsky, Ion Exchange I.
15. D. Reichenberg and D.J. Mc. Canley, J. Chem. Soc. 2731 (1955), J.A. Marinsky, Ion Exchange I.
16. K. Bunzl, J. Soil Sci. 25, 517 (1974).
17. P.I. Belkevich, K.A. Gayduk and L.R. Chistova, 6th International Peat Congress ' Peat and Peatlands in the Natural Environment Protection', Poznan 328 (1976).
18. K. Bunzl, J. Soil Sci. 25, 343 (1974).
19. B. Coupal and J.-M. Lalancette, Water Res. 10, 1071 (1976).
20. M.M. Kononova, Soil Organic Matter, Pergamon Press, London 47 (1966)
21. M. Schnitzer, Agrochimica 22, 216 (1978)
22. K. Bunzl, Z. Phys. Chem. 75, 118 (1971)
23. V. Puustjärvi, Acta Agric. Scand. 6, 410 (1956)



24. G. Lettinga, Biotechnol. Bioen. 22, 699 (1980).
25. H. Bergseth, Acta Agric. Scand. 28, 101 (1978).
26. F.E. Broadbent and G.R. Bradford, Soil Sci. 74, 447 (1952).
27. B. Sapek, 6th International Peat Congress ' Peat and Peat-lands in the Natural Environment Protection', Poznan 236 (1976).
28. J. Tummavuori and M. Aho, Ympäristö ja Terveys 10, 173 (1979).
29. J. Tummavuori and M. Aho, Ympäristö ja Terveys 9, 149 (1978).
30. I.M. Kolthoff and R. Belcher, Volumetric Analysis III, Interscience Publishers INC. New York 146 (1957)
31. I.M. Kolthoff and J.J. Lingane, J. Am. Chem. Soc. 58, 2457 (1936).
32. M. Aho, Research work for the degree of licence of philosophy, (1980).
33. L.P. Hammet and C.T. Sottery, J. Am. Chem. Soc. 47, 142 (1925).
34. E.B. Sandell, Colorimetric Determination of Traces of Metals 3, Interscience , New York - London (1959)
35. K. Nessler, Chem.Zentr. 27, 529 (1856).
36. M.S. Sherman, Ind. Eng. Chem. Anal. Ed. 14, 182 (1942).
37. M. Aho and R. Suontamo, Program Exchange ISSN: 0308-0714 Central Program Exchange 2 (1981).
38. M. Aho ja J. Tummavuori, Symposium of Analytical Chemistry. Publications of the University of Kuopio 5 (1982).
39. M. Aho ja J. Tummavuori, Suo 35, 67 (1984).
40. B.K. Theng, J.R. Wake and A.M. Posner, J. Soil Sci. 102, 70 (1966).
41. M. Adhikari and G. Chakrabarti, J. Indian Chem. Soc. 1, 394 (1973).
42. A. Broido, J. Polym. Sci. A2 7, 1761 (1969)
43. A.W. Coats and J.P. Redfern, Nature 201, 68 (1964)
44. J. Tummavuori and R. Suontamo, Finn. Chem. Lett. 6, 176 (1979)
45. M. Aho ja J. Tummavuori, Suo 35, 47 (1984)
46. J.-M. Lalancette and B. Coupal, 4th International Peat Congress 4 213 (1972)

47. J. Tummavuori and M. Aho, Suo 31, 45 (1980)
48. H. Irwing and R.J. Williams, Nature 162, 746 (1948)
49. J. Tummavuori and M. Aho, Suo 31, 79 (1980)
50. V. Puustjärvi, Suo 12, 51 (1961)
51. E. Tommila, *Fysikaalinen Kemia 4*, Otava Helsinki (1969)
52. K. Bunzl, W. Schmidt and B. Sansoni, *J. Soil Sci.* 27, 32 (1976)
53. K. Ratsack and A. Jungk, *Z. Pflanzenernähr Dueng. Bodenk.* 104, 193 (1964)
54. A. Jungk, *Z. Pflanzenernähr Dueng. Bodenk.* 104, 206 (1964)
55. M.B. Colella, S. Siggia and R.M. Barnes, *Anal. Chem.* 52, 967 (1980)
56. V.A. Thorpe, *J. Assoc. Off. Agric. Chem.* 56, 154 (1973)
57. J. Tummavuori, M. Aho and S. Sironen, *Suo 34*, 13 (1983)
58. A. Sugii, N. Ogava and H. Hashizume, *Talanta 27*, 627 (1980)

## APPENDIX

Program "Turvecap" .

COMMENT: Calculation of a straight based upon the heights of the AAS-signals corresponding 5 - 10 standard solutions.

The data needed : \* The name of the cation  
\* The heights of the signals corresponding the strongest standard solution measured after each weaker standard = a sensor.  
\* The heights of the signals corresponding the weaker standards

The calculation : \* By the least squares method.

COMMENT: The initial data for adsorption calculations.

\* The concentration of the test solution ( $\text{mg}/\text{dm}^3$ )  
\* The atomic weight of the element  
\* The charge of the ion  
\* The code of the peat sample  
\* The dry matter content of the sample (%)  
\* The volume of the suspended water ( $\text{cm}^3$ )  
\* The volume of one effluent fraction ( $\text{cm}^3$ )  
\* The number of the fractions  
\* The dilution ratio  
\* The weight of the peat sample (g)

COMMENT: Determination of the concentrations in the effluent fractions using the calculated straight and the sensor standard. Every second signal to be needed is that of the sensor standard solution.

The data needed: \* The heights of the signals of effluent fractions (cm)  
\* The heights of the signals of sensor standard

COMMENT: Calculation of the points on the adsorption curve

Assumption: \* The water suspended with peat flows out first. Confirmed with anions of low adsorption ability.

Alarms:  
or unusual  
adsorption  
behaviour \* If the first fraction of effluent contains ions and if this fraction is less than the volume of suspended water  
\* If the effluent contains more ions than the test solution

Estimation: \* The capacity by extrapolating the adsorption curve to  $y=0$ . The integrated area between the axis and curve corresponds to the capacity. The capacity is calculated more precisely by the

Program "Curvecomp".

COMMENT: The program calculates the exact capacity by integrating the area between the axis and the adsorption curve and follows the shape of descending region of the curve by calculating stepwise the values of  $K_{\text{comp}}$ .

The data needed: \* The number of integration steps  
\* The magnitude of the step ( meq/100g peat)  
\* The adsorption percentage corresponding each step (%)

CALCULATION: \* The ion exchange capacity ( meq/100 g peat )  
\* The values of  $K_{\text{comp}}$  stepwise

$$K_{\text{comp}} = \frac{M \times L}{\bar{M}}$$

M = concentration of free cation in the solution ( meq/dm<sup>3</sup> )  
 $\bar{M}$  = concentration of bound cation (meq/100gpeat)  
L = concentration of free adsorption places in the sample (meq/100 g peat)  
( calculated capacity minus amount adsorbed at a given time)

PRINTOUT: Stepwise mode. The final value of  $\log K_{\text{comp}}$  is calculated manually from the values at a 'constant' region.

Program "Turvekin".

COMMENT: The program calculates the degree of fit between the descending part of the adsorption curve and the first order kinetic equation.

The data needed: 12 points (x (meq/100g peat), y (%)) representing the definite adsorption curve.  $\Delta y$  of the points is 5 %, and the adsorption region is 80% - 20%



CALCULATION:

According to the equation

$$\log (a-x) = -\frac{K_{kin}}{2.3} t + C$$

a = initial concentration (meq/dm<sup>3</sup>)

x = reduction in concentration at the time t (meq/dm<sup>3</sup>)

$K_{kin}$  = reaction rate constant

The slope, cut, regression coefficient,  $K_{kin}$  and half-life is calculated using four groups of points by least squares method. The selected value of  $K_{kin}$  corresponds usually the maximum regression. If the regressions obtained with two groups of points are nearly equal, the selected value of  $K_{kin}$  represents the larger group.